The Effect of Recyclate Geometry on the Properties of Recycled Flake Reinforced Thermoset Composites

Kelsi M. Hurley

A thesis

submitted in partial fulfillment of the

requirements for the degree of

Master of Science in Materials Science and Engineering

University of Washington

2012

Committee:

Brian D. Flinn

Rajendra K. Bordia

K.Bhagwan Das

Pete E. George

Program Authorized To Offer Degree:

Materials Science and Engineering

TABLE OF CONTENTS

LIST OF FIGURES

LIST OF TABLES

ACKNOWLEDGMENTS

I would first like to acknowledge The Boeing Company for providing the funding for this research.

This thesis would not have been completed without the help and support of many individuals. I would like to express my sincere gratitude to all those who contributed to my research or provided support along the way:

Brian Flinn, for being an excellent research adviser and for providing insight and guidance throughout both my undergraduate and graduate studies.

Pete George, for first introducing me to the field of composites recycling and for providing guidance and direction to this project as the Boeing focal.

Aaron Capps, Brian Head, Alex O'Connor, Robert Timmerman, and Dzung Tran, for their help with laminate fabrication, mechanical testing, and data analysis.

All the members of the Flinn Group whom I have interacted with over the past few years. I could not have asked for a better graduate experience, and much of this I owe to them.

DEDICATION

To my parents

Chapter 1: Background

1.1 Introduction

Over the past few decades, the use of carbon fiber reinforced plastic (CFRP) composites has increased dramatically across a variety of industries. Composites are advantageous over many traditional materials because of their high specific properties and the ease by which such properties can be manipulated. This is especially true in aerospace, where the use of lighter, stronger, stiffer materials can reduce the weight of an aircraft and thus also reduce fuel consumption. Additional advantages of composite use in aerospace include improved fatigue and corrosion resistance, as well as lowered part counts and reduced maintenance. Many of these advantages contribute to reduced environmental impact during the service lifetime of a composite aircraft. However, there is currently no satisfactory method for recycling composite materials after they have exceeded their useable lifetime, regardless of their original application.

Recycled composites remain inferior to composites fabricated with virgin fibers for several reasons. Most recycling methods require removal of the matrix followed by reclamation and reimpregnation of the fibers. Each of these processes has inherent difficulties due to the crosslinked nature of thermoset polymers and the complex processing requirements for composite materials. Realistically, recycled composites can be expected to achieve comparable performance to sheet molding compounds or random short fiber composites fabricated with virgin fibers if fiber volume fractions can be improved without significantly reducing fiber length. One potential way to achieve this is to reinforce recycled laminates with flakes of shredded or single ply CFRP. The original matrix is left intake in the flakes, which preserves the local fiber orientation within the laminae of the original composite. This is expected to allow high fiber volume to be maintained and to prevent fiber damage during the fabrication of recycled laminates.

This thesis investigates the effect of recyclate geometry on recycled flake reinforced composites. This was accomplished by first producing CFRP flake reinforced laminates with either epoxy or vinyl ester matrices using vacuum assisted resin transfer molding (VARTM). The laminates were reinforced with either shredded flakes or single ply flakes. The shredded flakes were provided as-shredded by The Boeing Company, while the single ply flakes were cut from individual plies of cured unidirectional Toray T800S/3900-2 carbon fiber/epoxy tape. Flake size and aspect ratio

were varied among the laminates fabricated with the single ply flakes, while the geometry of the shredded flakes remained unmodified. Specimens from both types of laminates were then characterized and tested in flexure and tension.

1.2 Current Recycling Technologies

A variety of CFRP recycling technologies have been developed, most of which require thermal processing to remove the matrix material. These include heated chemical dissolution, pyrolysis, supercritical degradation, and a fluidized bed process. Each of these methods has distinct disadvantages and yields a fiber form that is difficult to process into high performance recycled components *(1,2)*. Reclaimed fibers can be fabricated into random short fiber composites, but low volume fractions remain a considerable problem. Although large compaction forces can be used to produce random laminates with fiber volume fractions as high as 40%, a majority of the fibers in these laminates are broken to lengths less than the critical length *(3)*. Thus, maximum load bearing capabilities cannot be attained. Alignment processes have also been used to produce mats of recycled carbon fiber. However, the low areal weights of these aligned mats *(4)* necessitate excessive processing to fabricate high quality recycled laminates. This areal weight barrier currently prohibits these recycled composites from being able to compete on a cost or performance basis with comparable composites fabricated with virgin fibers.

Mechanical processes have also been used to recycle composites, but most research has been focused on glass fiber reinforced composites. The recyclate is typically reduced to powder by several comminuting processes and then used in low loading levels as a filler material in sheet or bulk molding compounds *(2)*. Although these processes are successful, they do not take advantage of the properties of the original fibers. The use of comminuted carbon fiber composites as fillers would result in an even greater loss of high value fibers. Coarser pieces of recycled glass fiber composites have also been added to plastic lumber and asphalt *(5)*. As far as we know, no such applications for CFRP have been reported. This is likely because the abrasive nature of the carbon fiber makes it much more difficult to mechanically comminute carbon fiber reinforced composites.

1.3 Proposed Recycling Alternative

We propose that many of the current shortcomings in composites recycling can be overcome by fabricating random, locally aligned recycled laminates out of flakes of cured CFRP. If the orientation of the lamina can be preserved throughout the entire recycling process, it should be possible to fabricate random, recycled laminates with localized alignment, high fiber volume fractions, and nearly zero fiber damage. It has been shown that pyrolyzed single ply flakes of microwave delaminated CFRP can be recycled into a laminate with a tensile modulus comparable to that of a sheet molding compound fabricated with virgin material *(6)*. We propose that high quality recycled laminates can be produced without removing the original matrix from the flake material. Retaining the original matrix is expected to reduce the amount of additional resin required during future processing steps, help retain the mechanical properties of the original matrix and the fiber-matrix interface, result in less degradation of fiber properties during recycling, and promote easy handling of the intermediate material. Residual char left over from pyrolysis of the previously mentioned delaminated flakes has also been attributed to intraply porosity in recycled laminates fabricated with such material *(6)*. Therefore, retaining the resin in the flake material is expected to eliminate this problem as well.

The flakes of cured CFRP could be flakes of cured prepreg scrap, flakes of delaminated CFRP, or shredded flakes. Prepreg scrap would be cured prior to making flakes and fabricating a new laminate. This would ensure that the local fiber orientations were preserved during subsequent processing steps, as well as produce a reinforcement material with more consistent properties since the out time of the prepreg scrap would be uncontrolled. Most prepregs are cured at either 121˚C (250˚F) or 177˚C (350˚C). Thus, low temperature curing resin systems would not be an option for laminates fabricated with uncured flakes. Curing the prepreg before making flakes would also allow for the use of peel ply as a potential surface preparation to promote adhesion between the flakes and the new matrix.

Fabricating laminates with delaminated or shredded flakes of CFRP would be an option for recycling cured parts. Both processes will need to be optimized, but may become feasible options in the near future. Conventional pyrolysis and microwave assisted pyrolysis have both been used to separate a cured composite into individual lamina *(6)*. Although pyrolysis removes much of the original matrix, other delamination methods may be possible. Grinding and sifting has been

used to reduce cured CFRP into small fragments less than 5.5 mm *(7)*. It's possible that an optimal shredding process that produces larger, flake-like pieces of a desired geometry could be developed. As of yet, the ideal size and geometry of such optimal shredded flakes is unknown. Studying the properties of laminates fabricated with either single ply flakes or the as-shredded material provided by The Boeing Company should provide insight into this.

1.4 Engineered Wood Products

1.4.1 Morphology

The morphology of our flake reinforced recycled CFRP laminates is similar to that of engineered wood products such as flakeboard and oriented strand board (OSB) that consist of thin wooden strands bonded together with resin. Engineered wood products fabricated with random strands may be referred to as particle board, chipboard, flakeboard, strandboard, or waferboard depending on the type of classification and the size and shape of the wood strands *(8)*. These products typically consist of randomly oriented strands, whereas OSB consists of either a randomly oriented or an aligned strand core and aligned outer layers. In this thesis, engineered wood products fabricated with random strands will be referred to as flakeboard. Figure 1 below illustrates the physical differences between OSB and flakeboard.

Figure 1: Comparison between OSB and flakeboard (or waferboard) ***(9)***

1.4.2 Fabrication

To fabricate OSB, debarked logs go through a stranding process that slices them into long, thin strands in the direction of the wood grain *(10)*. The strands are of uniform length and thickness, and are typically 10.16 to 15.24 cm (4 to 6 in) long, 1.27 to 2.54 cm (.5 to 1 in) wide, and .07 cm

(.03 in) thick *(11)*. After stranding is complete, the strands are either stored in wet bins or sent directly to a dryer. Dry strands are sent to rotating blender and mixed with two different additives: wax and resin binder. The wax and resin are typically added at approximately 6% by weight, with the wax being no more than 1.5% by weight *(11, 12)*. The wax is added to improve the moisture resistance of the final product and to promote favorable interactions between the resin and the strands during processing *(12)*. The resin binder must also have excellent moisture resistance, and different resin systems may be used for the core and outer layers of the OSB *(11)*. Phenolic resins or isocyanate binders are the most common resin binders used *(13)*.

After the strands are coated with resin binder and wax they are sent to mat formers that orient the strands on top of a moving conveyor belt. This orientation is accomplished by dropping the strands through an array of spinning discs or troughs just above the belt. The orientation is controlled by the spacing of the discs; the long, narrow strands must become oriented in a specific direction in order to fall through the disc array to the belt. Strand layers of different orientations are deposited subsequently on top of one another, and the moving conveyor carries the loose strand mat to a hot press once all the layers are deposited. The mat is then pressed at elevated temperatures to consolidate the mat and cure the resin. Mats are typically consolidated at 177 to 204°C (350 to 400°F) for 3-5 minutes *(11)*. Finally, the consolidated mats are cut and stacked. Figure 2 below illustrates the complete OSB manufacturing process.

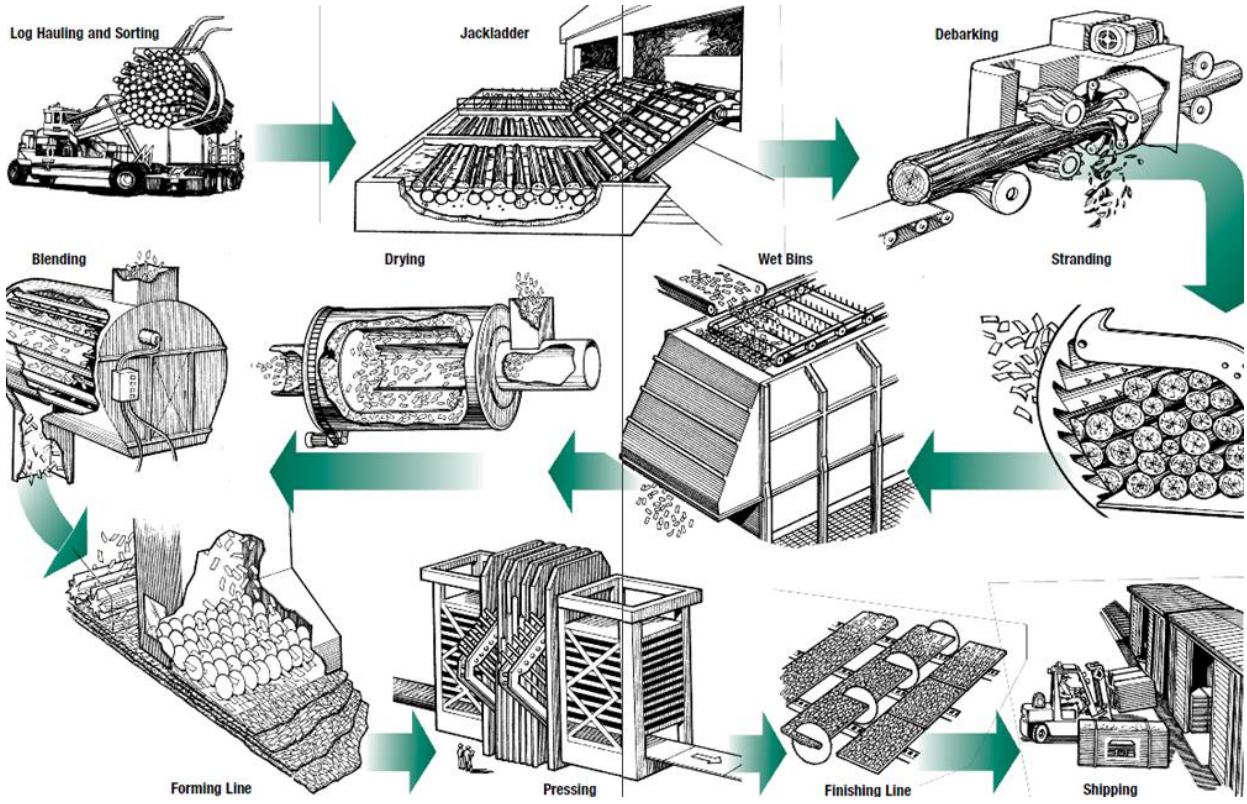

Figure 2: OSB manufacturing process *(11)*

Although the recycled flake reinforced CFRP laminates in this study were random and thus more like flakeboard, laminates with a structure more analogous to OSB could be fabricated as well. Once the desirable properties and geometries of the CFRP flakes are determined, a similar process modeled after the OSB fabrication process could likely be developed to fabricate recycled flake reinforced CFRP laminates. The laminates could be made up of oriented layers or be completely random. For the purpose of this study, random quasi-isotropic laminates were the most desirable. OSB is intended to mimic structural plywood and needs the high bending strengths provided by the oriented outer layers *(14)*. Recycled laminates reinforced with cured CFRP flakes would be intended for low load bearing applications that require equal properties in all directions.

1.4.3 Optimum Strand Characteristics

For OSB, one of the primary requirements is high bending strength. Post *(15)* determined that this property was dependent on both flake length and thickness. Bending strength was found to

increase with increasing strand length up to a length of 10.16 cm (4 in), but decrease with increasing strand thickness. Post *(16)* also determined that bending strength increases with increasing length-to-thickness ratios up to a ratio of at least 300, and that this ratio is a better indication of flakeboard quality than either dimension is independently. Brumbaugh *(17)* determined that the optimum length-to-thickness ratio is between 150 and 250, and also correlated flake geometry with OSB properties. Long flakes were again found to improve bending strength, while long, thin flakes were shown to promote dimensional stability and short, thick flakes were shown to have better internal bonding. Long strands are also necessary to achieve a high degree of orientation through the spinning discs and thus higher directional strength properties *(18)*. The same bending and orientation requirements do not apply to the random laminates fabricated in this study. However, flake reinforced CFRP laminates are expected to show similar property dependences on flake length and flake geometry based on their morphological similarities to OSB and flakeboard.

1.4.4 Failure Modes

Four orientation-dependent failure modes have been identified for random flakeboard tested in tension *(19)*. These include transverse/shear failure, rolling shear failure, tension failure, and disbonding. Transverse/shear failure in which the flakes fail along the wood fiber occurred in flakes with a grain orientation more than 10 degrees offset from the loading direction. This was the most commonly observed failure mode because most of the flakes in a random flakeboard are not aligned with the loading direction. Tensile failure characterized by long splintered flake ends occurred in the flakes with grain orientations that were nearly aligned with the loading direction. Rolling shear failure in which the fibers fail perpendicular to the loading direction occurred in flakes that were almost perpendicular to the applied load. These flakes also tended to be surrounded by other low angle flakes. The final failure mode observed was flake disbonding. This failure mode was observed for flakes oriented less than 45 degrees from the loading direction and with low flake-to-flake bond strength and/or high flake strength. These failure modes are consistent with the type of failures we would expect to see in our single ply flake reinforced laminates. If the unidirectional flakes are oriented parallel to the applied load, fiber failure should occur as long as there is good bonding between the flakes and the matrix. As the degree of flake orientation increases away from the direction of the applied load, fiber failure should decrease and failure in the flake matrix along the fiber direction should become more

prevalent. Disbonding is very undesirable, but is also a potential failure mode. If bonding is especially poor between the flakes and the matrix, then disbonding could be the only failure mode observed. Additional failure modes are possible for the laminates fabricated with shredded flakes. These flakes could also delaminate or fail intralaminarly within a ply.

1.5 Prediction of Composite Properties

The flake reinforced laminates fabricated in this study are comprised of well-packed regions of short fibers. Thus, in addition to the demonstrated behavior of OSB and flakeboard, well-established models for short fiber composites should also provide insight into the mechanical behavior of flake reinforced CFRP composites. Most models have been found to accurately predict the properties of aligned short fiber composites, but could likely be modified to account for random flake orientation.

1.5.1 Critical Length

In short fiber reinforced composites, the fibers must be sufficiently long such that stress can be effectively transferred from the matrix to the fibers. One of the most common theories of stress transfer in aligned short fiber composites is the shear lag analysis developed by Rosen *(20)*. According to this model, force equilibrium on an infinitesimal length of fiber can only occur if shear stress is present at the fiber matrix interface, as shown below.

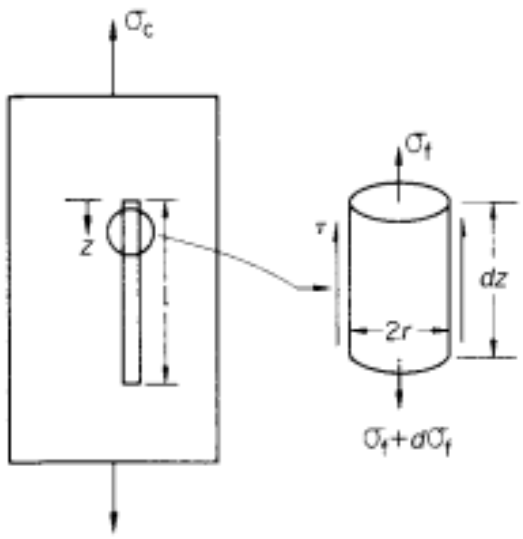

Figure 3: Equilibrium of a small length of fiber in a short fiber composite *(21)*

By balancing the forces on an infinitesimal length of fiber, integrating with respect to the z direction to find the stress experienced by the fiber, and making appropriate assumptions about the interfacial shear stress and the maximum stress that can be attained in the fiber, the critical length, l_c, can be expressed by the following equation:

$$l_c = \frac{\sigma_{fu} d}{2\tau} \qquad \text{[Equation 1]}$$

where σ_{fu} is the ultimate strength of the fiber, d is the diameter of the fiber, and τ is the matrix yield stress in shear or the fiber-matrix bond strength in shear, whichever is lower.

The critical length is defined as the minimum fiber length in which the ultimate strength of the fiber can be attained. If the length of the fiber is less than the critical length, then the fiber will never experience its ultimate strength, regardless of the applied stress. The fiber-matrix interface will fail instead, and fiber pullout will be the failure mode instead of fiber fracture. In an ideal composite, failure would occur when all the fibers in a cross section had failed because the matrix would be unable to sustain the load.

Equation 1 is only valid for aligned short fiber laminates. However, it is expected that a modified shear-lag model could be applied to random flake reinforced laminates by accounting for geometry and using effective properties to account for flake orientation. Such a model would yield a critical flake length instead of a critical fiber length. Knowing this critical flake length would be essential for fabricating flake reinforced laminates that achieve the maximum possible performance.

1.5.2 Prediction of Strength

Based on the shear-lag model described above, the strength of an aligned short fiber composite with fibers greater than the critical length is given by the following equation:

$$\sigma_{cu} = \sigma_{fu}\left(1 - \frac{l_c}{2l}\right)V_f + \sigma_{m^*}V_m \qquad \text{[Equation 2]}$$

where l is the length of the fiber, V_f and V_m are the volume fractions of the fibers and matrix, respectively, and σ_{m^*} is the stress in the matrix at the fracture strain of the fibers. As the fiber length increases, the strength of the composite approaches that of a continuous composite of equivalent volume fraction.

Equation 2 is simply a modified version of the rule of mixtures, which assumes that the constituents of a composite contribute properties to the composite that are proportional to their respective volume fractions. In order for this to be the case, the fibers must be perfectly oriented, of uniform strength, have no edge effects, and be perfectly bonded to the matrix *(21)*. For random short fiber composites, predictions of strength become much more complicated.

Several models have been proposed to predict the strength of random short fiber composites. Many models are simply modified versions of the rule of mixtures that include extra coefficients in the first term to account for fiber length and orientation effects. Models of this form have been proposed by Blumentritt and Cooper, Curtis et al., Kelly and Tyson, and Chiang. Other models for predicting the strength of random short fiber composites based on various failure criteria have been developed independently by Chen, Baxter, and Hahn *(22)*.

No one single theory that has been proven completely accurate for predicting the strength of all types of random short fiber composites. Such a theory would need to account for all the factors that influence the strength of a random short fiber composite, as well as the complex interactions between them. Developing a model to predict the strength of random flake reinforced composites would be even more difficult.

1.5.3 Prediction of Modulus

For composite materials, elastic modulus can usually be predicted by either the rule of mixtures equations or the Halpin-Tsai equations. There are two forms of each type of equation: one for the plane strain condition in which the load is applied parallel to the fibers (longitudinal form), and one for the plane stress condition in which the load is applied perpendicular to the fibers (transverse form). Since these equations are based on either plane strain or plane stress, they are most applicable to aligned fiber composites. The rule of mixtures equations are given below:

Longitudinal rule of mixtures (LROM):

$$E_L = E_f V_f + E_m V_m \quad \text{[Equation 3]}$$

where E_L is the elastic modulus of the composite in the longitudinal direction, and E_f and E_m are the elastic moduli of the fibers and the matrix, respectively.

Transverse rule of mixtures (TROM):

$$E_T = \frac{E_f E_m}{E_f V_m + E_m V_f} \quad \text{[Equation 4]}$$

where E_T is the elastic modulus of the composite in the transverse direction.

Halpin and Tsai modified the rule of mixtures equations to account for fiber discontinuities and fiber packing. The general form of the Halpin-Tsai equation is given below:

$$E_c = \frac{E_m[1+\xi\eta V_f]}{1-\eta V_f} \qquad \text{[Equation 5]}$$

with

$$\eta = \frac{(E_f/E_m)-1}{(E_f/E_m)+\xi} \qquad \text{[Equation 6]}$$

where ξ is a measure of the reinforcement geometry that depends on loading conditions. For an aligned short fiber composites, Halpin and Tsai suggested that ξ=$2l/d$ for the longitudinal case and $\xi = 2$ for the transverse case. Equations 5 and 6 can also be applied to lamellar shaped tape reinforcements when ξ=$2l/t$ for the transverse case and ξ=$2w/t$, where l is the length of the tape in the 1 direction, t is the thickness of the tape in the 3 direction, and w is the width of the tape in the 2 direction *(23)*. Based on the applicability of the Halpin-Tsai equations to aligned reinforcements of various geometries, the idea of a modified Halpin-Tsai equation to predict the elastic modulus of an aligned flake reinforced composite is quite plausible if E_f is taken as the modulus of the flake instead of the modulus of the fiber.

The following empirical equation proposed by Lavengood and Goettler give the elastic modulus of a random short fiber composite with random planar fiber orientation as a function of the longitudinal and transverse moduli of an aligned short fiber composite of the same composition and fiber volume fraction *(24)*:

$$E_{random} = \frac{3}{8}E_L + \frac{5}{8}E_T \qquad \text{[Equation 7]}$$

Lavengood and Goettler also proposed a similar empirical equation for a random three dimensional fiber orientation:

$$E_{random} = \frac{1}{5}E_L + \frac{4}{5}E_T \qquad \text{[Equation 8]}$$

The Halpin-Tsai equations for aligned flake reinforced composite may be useful for random flake reinforced composites if Equations 7 and 8 hold true for this class of composites as well. Since flake reinforced laminates may not have perfectly planar reinforcement, an equation more similar to Equation 8 may be most appropriate.

The above models for predicting the moduli of short fiber composites have also been applied to flakeboard, but with limited success. Shaler and Blankenhorn *(25)* suggested a modified version of the Halpin-Tsai equations that accounted for flake geometry, flake orientation, density, resin content, and wood species. However, their model underestimated the elastic moduli of several types of flakeboards by 25%. Hunt et al. applied the longitudinal rule of mixtures to flexural properties and achieved predictions of the flexural strength and flexural modulus of flakeboard that were within 10% of the experimental values *(25)*.

1.6 Existing Flake Reinforced CFRP Composites

As far as we know, no flake reinforced laminates have been fabricated with cured composite material. In one study, cured carbon fiber/epoxy prepreg scrap was successfully incorporated into a high density polyethylene (HDPE) matrix to improve the performance of structural lumber. However, although the cured prepreg was initially cut into .5 cm by 1 cm (.2 in by .4 in) flakes, it was subsequently fed through a screw extruder along with the HDPE with the intention of tearing up the prepreg and exposing as many individual fibers to the matrix material as possible *(26)*.

Several flake-form molding compounds fabricated with flakes of virgin prepreg are commercially available. These include Hexcel HexMC®, Hexcel HexTOOL™ M61, Quantum Composites Lytex®, and several types of TenCate Compression Molding Compounds. These

materials can achieve properties comparable to those of comparable continuous fiber quasi-isotropic laminates fabricated with fabric prepreg *(27)*. Figure 4 below shows the typical flake architecture of these products.

Figure 4: HexMC™ sheet molding compound *(28)*

In addition to the prepreg based materials such as that shown in Figure 4, another comparable commercial material is Zoltek Panex® 35, an unimpregnated flake-type chopped fiber.

Flake-type material similar to HexMC® has also been fabricated with virgin prepreg and studied by the Feraboli group *(29)*. This material is referred to as a prepreg-based discontinuous carbon/epoxy system, and it is essentially identical in structure to HexMC®. Since all of these flake reinforced materials are fabricated with high quality prepreg (except Zoltek Panex® 35), they represent an upper bound on the performance we could expect to achieve by incorporating cured CFRP flakes in a secondary matrix.

Chapter 2: Materials and Methods

2.1 Research Approach

To evaluate the effect of flake geometry on the properties of recycled flake reinforced CFRP composites we fabricated several laminates with different flake characteristics. Both single ply flakes made in the laboratory and shredded flakes provided by The Boeing Company were used as the reinforcement. The geometry of the shredded flakes was highly variable, while the geometry of the single ply flakes was very uniform. Optical microscopy was performed on both types of flakes to analyze and compare their physical characteristics. All the laminates in this study were fabricated using VARTM and machined flat once they were fully cured.

Six 15.2 cm by 15.2 cm (6 in by 6 in) laminates with random flake orientation were fabricated first. These small laminates were fabricated to evaluate the chosen resin infusion process, to determine a single matrix resin type to use for future laminates, and to get an initial idea of the physical and mechanical properties of the flake reinforced laminates. Of these six laminates first fabricated, two were fabricated with 1.27 cm by 1.27 cm (.5 in by .5 in) single ply flakes as the reinforcement. One was infused with epoxy, while the other was infused with vinyl ester. The other four laminates were fabricated with shredded flakes as the reinforcement. Two were fabricated with epoxy and two were fabricated with vinyl ester. In one of the shredded flake/epoxy laminates and one of the shredded flake/vinyl ester laminates, the shredded flakes were washed with acetone and fully dried prior to resin infusion. This was done to determine whether the fines present in the shredded flakes would inhibit bonding between the matrix and the flakes. Each of the six 15.2 cm by 15.2 cm (6 in by 6 in) laminates was tested in flexure.

Next, six 25.4 cm by 25.4 cm (10 in by 10 in) laminates with random flake orientation were fabricated. All of these larger laminates were infused with vinyl ester resin. Five of these laminates were fabricated with single ply flakes of varying aspect ratios (length to width ratios) as the reinforcement. The aspect ratio was varied between 1:1 and 1:4 while either flake area was held constant at 1.61 cm^2 (.25 in^2) or flake length was held constant at 2.54 cm (1 in). These laminates were fabricated to test the effect of single ply flake geometry on the mechanical properties of recycled flake reinforced laminates. One 25.4 cm by 25.4 cm (10 in by 10 in) laminate was fabricated with shredded flakes as the reinforcement. This laminates was fabricated

to evaluate the mechanical properties of recycled shredded flake reinforced laminates, and to compare the properties of recycled shredded flake reinforced laminates with those of recycled single ply flake reinforced laminates. Each 25.4 cm by 25.4 cm (10 in by 10 in) laminate was tested in both tension and flexure. The failure modes of these laminates in both flexure and tension were assessed by analyzing the failure surfaces of the tested specimens. Digital image correlation (DIC) was used during tensile testing of the single ply flake reinforced laminates to gain additional insight into their stress-strain behavior in tension.

An additional 15.2 cm by 15.2 cm (6 in by 6 in) laminate was fabricated with single ply flakes as the reinforcement and vinyl ester as the matrix. The flakes were aligned by hand in the mold instead of being randomly scattered. This laminate was then tested in flexure to compare the experimental flexural modulus with that predicted by the longitudinal rule of mixtures. A larger laminate that could be tested in tension would have been desirable. However, aligning the flakes by hand was extremely time-intensive and difficult. Furthermore, based on the agreement between the predicted and flexural modulus of flakeboard, as described in section 1.5.3, and the morphological similarities between flakeboard and our recycled flake reinforced composites, the flexural modulus of a single ply flake/vinyl ester laminate would be expected to agree with the predicted value. A 15.2 cm by 15.2 cm (6 in by 6 in) laminate was therefore a logical first step towards assessing whether the properties of flake reinforced laminates can be predicted by models developed for other types of composites.

Optical microscopy was performed on each of the 25.4 cm by 25.4 cm (10 in by 10 in) laminates to assess flake distribution and laminate quality. The densities of these laminates were measured as well so that flake and fiber volume fractions could be determined.

Each of the aforementioned research steps is discussed in greater detail within this chapter. Table 1 below provides a description of each of the laminates fabricated in this study as well as the type of mechanical testing that was performed on each.

Table 1: Laminate descriptions

Laminate	Flake Type	Matrix	Laminate Size (cm x cm)	Laminate Size (in x in)	Flake Orientation	Flake Size (cm by cm)	Flake Size (in by in)	Aspect Ratio	Tested in Flexure	Tested in Tension
1	Single Ply	Vinyl Ester	15.2 x 15.2	6 x 6	Random	1.27 x 1.27	.5 x .5	1:1	Yes	No
2	Single Ply	Epoxy	15.2 x 15.2	6 x 6	Random	1.27 x 1.27	.5 x .5	1:1	Yes	No
3	Shredded Flakes	Vinyl Ester	15.2 x 15.2	6 x 6	Random	As-shredded	As-shredded	N/A	Yes	No
4	Shredded Flakes	Epoxy	15.2 x 15.2	6 x 6	Random	As-shredded	As-shredded	N/A	Yes	No
5	Shredded Flakes Washed in Acetone	Vinyl Ester	15.2 x 15.2	6 x 6	Random	As-shredded	As-shredded	N/A	Yes	No
6	Shredded Flakes Washed in Acetone	Epoxy	15.2 x 15.2	6 x 6	Random	As-shredded	As-shredded	N/A	Yes	No
7	Single Ply Flakes	Vinyl Ester	25.4 x 25.4	10 x 10	Random	1.27 x 1.27	.5 x .5	1:1	Yes	Yes
8	Single Ply Flakes	Vinyl Ester	25.4 x 25.4	10 x 10	Random	.89 x1.78	.35 x .7	1:2	Yes	Yes
9	Single Ply Flakes	Vinyl Ester	25.4 x 25.4	10 x 10	Random	.64 x 2.54	.25 x1	1:4	Yes	Yes
10	Single Ply Flakes	Vinyl Ester	25.4 x 25.4	10 x 10	Random	1.27x 2.54	.5 x 1	1:1	Yes	Yes
11	Single Ply Flakes	Vinyl Ester	25.4 x 25.4	10 x 10	Random	2.54 x 2.54	1 x 1	1:2	Yes	Yes
12	Shredded Flakes	Vinyl Ester	25.4 x 25.4	10 x 10	Random	As-shredded	As-shredded	N/A	Yes	Yes
13	Single Ply	Vinyl Ester	15.2 x 15.2	6 x 6	Aligned	1.27 x 1.27	.5 x .5	1:1	Yes	No

2.2 Materials

2.2.1 Single Ply Flakes

Single plies of unidirectional Toray T800S/3900-2 carbon fiber/epoxy tape were surface prepared with Precision Fabrics 60001 polyester peel ply on both sides, vacuum bagged, and cured in an autoclave. The autoclave cure cycle was as follows:

- Heat to 57.2°C (135°F) at a rate of 1.1°C/min (2°F/min), increase pressure to 0.6 MPa (89 psi) at a rate of 0.1 MPa/min (20 psi/min), soak for 0 min

- Heat to 177°C (350°F) at a rate of 5.6°C/min (10°F/min), maintain pressure of 0.6 MPa (89 psi), soak at 177°C and 0.6 MPa for 120 min (2 hr)
- Cool to 10°C (50°F) at a rate of 5.6°C/min (10°F/min), maintain pressure of 0.6 MPa (89 psi), soak for 0 min
- Decrease pressure to 0 Mpa (0 psi) at a rate of 0.1 MPa/min (20 psi/min), while maintaining a temperature of 10°C (50°F), soak for 0 min

Once the single plies were cured, the peel ply was removed from both sides. Care was taken when removing the peel ply to ensure that the cured unidirectional plies did not crack or split along the length of the fibers. Any cracked or split regions were discarded. Gloves were worn at all times when removing the peel ply or handling the bare CFRP afterwards. The cured plies were then sheared into strips of the desired length (in the direction of the fibers) using a foot-powered squaring shear. The shear was cleaned with acetone prior to every use. The sheared strips were collected on a plastic sheet behind the blade so that they would not fall to the floor. These strips were then cut into flakes of the desired width (perpendicular to the direction of the fibers) by hand with a razor blade. Flakes of the same geometry were stored together in sealed plastic bags until the laminates were fabricated.

2.2.2 Shredded Flakes

Shredded flakes were provided as-shredded by The Boeing Company. The specifications of the shredding process were not provided. The flakes all originated from cured Toray T800S/3900-2 CFRP parts. Besides washing the flakes for two of the laminates with acetone, no further processing of the flakes was done prior to resin infusion. The shredded flakes varied in length, width, thickness, and overall geometry, as seen below in Figure 5.

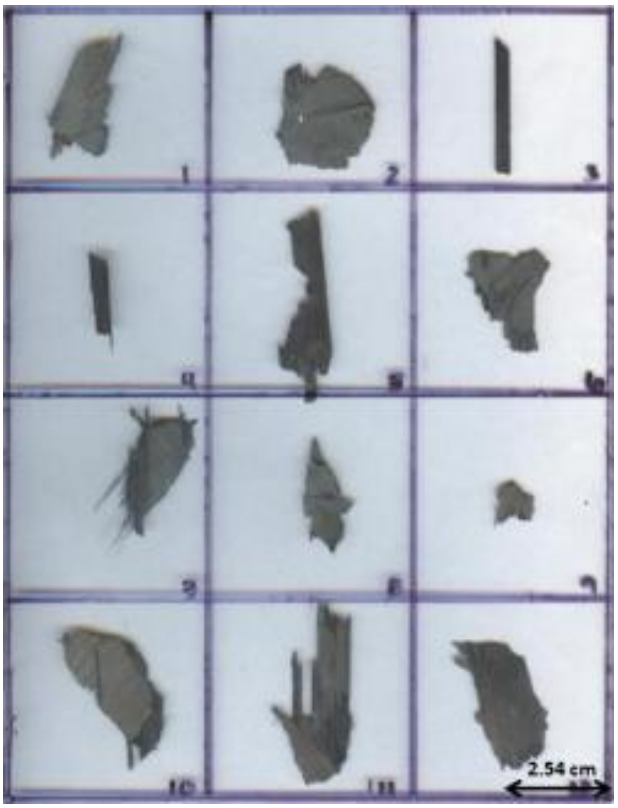

Figure 5: Random selection of shredded flakes

Figure 6 below shows the shredded flakes in the as-shredded condition they were received in.

Figure 6: Shredded flakes in the as-shredded condition

The shredded flakes also contained several types of contaminants such as wire, paper, wood, and twine. These contaminants were removed prior to laminate fabrication because it was assumed that they would not be introduced during an optimum shredding process. The most common contaminants found in the shredded flakes are shown below in Figure 7.

Figure 7: Common contaminants found in the shredded flakes

2.2.3 Resin

Orca Composites Vinyl Ester 511 Resin for Infusion was chosen as the matrix resin for the majority of the laminates. This is a low viscosity, infusion grade vinyl ester that cures at room temperature with the addition of methyl ethyl ketone peroxide initiator (MEKP). A ratio of 1.5% initiator by weight was mixed with the resin. It was then mixed by hand for 3 minutes. At least 5 minutes were allowed to elapse between the end of mixing and the beginning of infusion to allow the resin to degas. Degassing under vacuum was not necessary because of the significantly low viscosity of the resin.

Orca Composites Pro Glas 1301 Epoxy Infusion Resin was used as the matrix resin for three of the laminates. This is a low viscosity, infusion grade epoxy that cures at room temperature with the addition of Pro-Glas Hardener. The hardener was added at a 4:1 ratio of resin to hardener. The resin and hardener were mixed by hand for 3 minutes and then degassed under vacuum for 10 minutes prior to infusion. This was necessary to remove the air bubbles that were introduced into the resin during mixing. Unlike the vinyl ester, the epoxy was not of low enough viscosity to degas by itself under ambient conditions.

2.3 Laminate Fabrication

All laminates were fabricated using VARTM. 1.27 cm (.5 in) tall square molds were cut from HDPE and used to contain the flake preforms. The molds were set on top of a caul plate wrapped in non-stick nylon bagging material. This caul plate was then set on a second caul plate wrapped in non-stick nylon bagging material. Nylon bagging material was chosen over release film because tacky tape adheres better to the bagging material. The inner caul plate was necessary to provide a flat tool side to each cured laminate. Since the bottom caul plate was wrapped with bagging material, once vacuum was pulled this bagging material would conform to the flake architecture at the bottom of the mold if there was not an inner caul plate. This would result in a finished laminate with an unsmooth bottom surface. The added inner caul plate was necessary because the vacuum was pulled between two sheets of bagging material, rather than between a caul plate and a top sheet of bagging material. An ideal mold would have been a two part metal mold with a picture frame top piece that could be attached to a flat bottom piece.

A flake preform was created by randomly scattering the flakes in the mold by hand. The flakes were dropped from a height of approximately 15.2 cm (6 in) so that they would fall randomly

into the mold. Some manipulation of preform was necessary to ensure uniform coverage in the mold cavity. 120 grams of flakes were used for each 15.2 cm by 15.2 cm (6 in by 6 in) flake preform, while 330 grams of flakes were used for each 25.4 cm by 25.4 cm (10 in by 10 in) flake preform.

Once the preform was made, the inlet and outlet tubes were secured on each side of the mold. Spiral tubing was attached to the inlet and outlet tubes and extended the entire width of the preform so that the resin would be pulled left to right across the entire length and width of the preform. The spiral tubing connected to the inlet tube was connected to the preform with flow media. The flow media extended from the spiral tubing down the left inner left edge of the mold. Four stacked sheets of peel ply were used to connect the right side of the preform to the spiral tubing connected to the outlet tube. Peel ply was chosen over flow media because it was found to provide the desired amount of resistance to resin flow so that the resin would backfill in the preform and not be pulled through it too quickly. One sheet of peel ply was placed over the entire preform so that it touched the spiral tubing on both sides of the mold. This was done to aid in resin flow across the entire laminate and to provide a barrier between the flakes and the vacuum bag to prevent the sharp corners of the flakes from poking holes in the bag.

Next, the vacuum bag was placed over the entire set up and tacky taped around the perimeter of the bottom caul plate. Pleating was necessary to ensure that the bag conformed around the set up and the preform. Any sharp edges or corners were covered in tacky tape to ensure that no holes were created in the bag during the infusion process. A vacuum of 30 mmHg was pulled on the laminate and released several times. This was expected to help nest the flakes in the preform prior to infusion and contribute to a well-consolidated laminate.

Next, the inlet tube was placed in the resin pot and the clamp on the inlet was released so that resin would be introduced into the preform. Resin flow was controlled so that it did not flow too quickly through the preform. The inlet tube was clamped shut once the preform was fully infused. A vacuum of 30 mmHg was pulled on the laminate until the resin hardened. The entire set up was then placed in an autoclave for 1 hour at 60°C (140°F) to post cure the laminate. This was done for both the epoxy and vinyl ester laminates.

A schematic of the typical VARTM set up used to fabricate each of the laminates in this study is shown below in Figure 8.

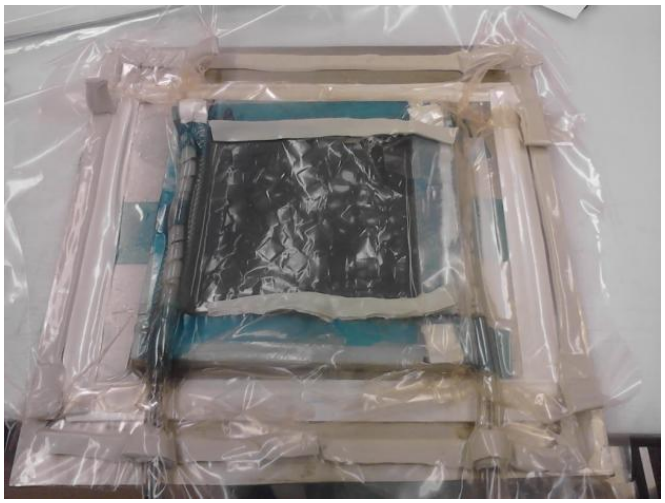

Figure 8: Typical VARTM set up used to fabricated each laminate

2.4 Surface Machining of the Laminates

The random scattering of the flakes and the absence of a top caul plate over the preforms resulted in laminates with non-flat top surfaces. These surfaces had to be machined to produce flat specimens for mechanical testing. Three different machining methods were used. The randomly oriented 15.2 cm by 15.2 cm (6 in by 6 in) laminates were ground flat on a DoAll MTA-70 Slicer/Grinder with an alumina grinding wheel. The aligned 15.2 cm by 15.2 cm (6 in by 6 in) laminate and one of the 25.4 cm by 25.4 cm (10 in by 10 in) laminates were machined flat in the mechanical engineering department's machine shop using a 3.18 cm (1.25 in) diameter indexable cutter with polycrystalline diamond (PCD) tipped inserts at 6,000 rotations per minute and a table speed of 38 cm (15 in) per minute with a full diameter radial depth of cut. The remaining 25.4 cm by 25.4 cm (10 in by 10 in) laminates were machined flat in the aeronautics and astronautics department's machine shop using 2.54 cm (1 in) diameter carbide tipped inserts at 700 rotations per minute and a table speed of 15.24 cm (6 in) per minute with a full diameter radial depth of cut. Constant water supply was used during machining to manage dust. The appropriate machining specifications were chosen by the individual machine operators. Identical

machining methods for all the laminates would have been most desirable. However, grinding on the DoAll MTA-70 Slicer/Grinder was impractically slow, and the equipment used in the mechanical engineering department's shop malfunctioned and could not be used to machine all the laminates.

2.5 Optical Microscopy of the Flake Reinforcement

Optical microscopy was performed on the shredded flakes and the 1.27 cm by 1.27 cm (.5 in by .5 in) single ply flakes to evaluate flake characteristics and to determine if microcracking occurred in the shredding flakes during the shredding process. Imaging was done at magnifications of 5, 10, and 20X with an Olympus BX51 microscope with attached Olympus SC30 digital camera. The flakes were mounted in epoxy resin and polished prior to imaging. Pink rhodamine B dye hydrated with acetone was added to the epoxy mounting resin at a concentration of .006 weight % in order to provide contrast between the matrix resin and the mounting resin. The flakes and mounting resin were cured in mounting cups in an autoclave at 66°C (150°F) and .6 MPa (85 psi) for 1 hour. Curing of the mounted flakes was done under pressure to force the mounting resin into any cracks that may be present in the flakes. The mounted specimens were then polished using successively smaller 15, 9, and 3 μm diamond abrasive on polishing wheels. The mounted shredded flakes were cut in half prior to polishing to expose the inner portions of the flakes.

2.6 Mechanical Characterization of the Flake Reinforced Laminates

2.6.1 Flexure

Flexure tests were performed on 5 specimens from each of the laminates specified in Table 1. Testing was done in accordance with ASTMD790 *(30)*, with two exceptions. The specimens from the 25.4 cm by 25.4 cm (10 in by 10 in) laminate fabricated with 1.27 cm by 1.27 cm (.5 in by .5 in) single ply flakes were tested with a 14:1 support span to depth ratio. The specimens could not be tested with the recommended 16:1 support span to depth ratio because they were not long enough for their thickness. Flexure data was obtained from only 3 specimens from the 15.2 cm by 15.2 cm (6 in by 6 in) shredded flake/vinyl ester laminate due to unexpected cross frame behavior during testing of the first two specimens.

All flexure specimens were 2.54 cm (1 in) wide, and all flexure tests were performed on an Instron 4505 load frame at a constant strain rate of .01 min^{-1}. All specimens were tested with the machined surface in tension and the tool surface in compression.

2.6.2 Tension

5 specimens from each of the 25.4 cm by 25.4 cm (10 in by 10 in) laminates were tested in tension in accordance with ASTM D3039 *(31)*. Recommended specimen dimensions for a random discontinuous laminate are 25.4 cm long by 2.54 cm wide (10 in by 1 in). However, the specimens tested in this study were 24.1 cm long by 2.72 cm wide (9.5 in by 1.07 in). The discrepancy in the length was due to the mold size. 25.4 cm by 25.4 cm (10 in by 10 in) was the largest mold size for which the chosen VARTM set up produced a well-infused laminate, and .64 cm (.25 in) was trimmed from each end. The error in the width was due to limited precision during cutting.

All specimens were tabbed with 8-ply woven fiberglass/epoxy tabs. 25.4 cm by 15.24 cm (10 in by 6 in) regions were cut out of each laminate, tabs were bonded on, and then individual specimens were cut from the tabbed laminates. The tabs were fabricated using VARTM and bonded to the tensile specimens with Henkel EA9394 room temperature cure two part paste adhesive. All bonding surfaces were sanded with 80 grit SiC paper for approximately 1 minute. The sanded surfaces were solvent wiped with acetone in successive passes until no more dust was visible on the wipes. The paste adhesive was mixed immediately after sanding and a thin layer was applied to the sanded regions on one side of each flake reinforced laminate with a wooden tongue depressor. The fiberglass tabs were then placed sanded side down on the adhesive. Several caul plates were stacked on the bonding laminates and left for 24 hours while the adhesive cured. After 24 hours had elapsed, the weight was removed and the process was repeated to bond tabs to the opposite side of each flake reinforced laminate. The tabbed laminates were then post cured in an autoclave at 66°C (150°F) for 1 hour.

After bonding was complete, the tabbed laminates were cut into tensile specimens using a DoAll MTA-70 Grinder/Slicer. All specimens were tested with an Instron 5585H load frame at a strain rate of .01 min^{-1}. Specimens were initially preloaded to 1.3 kN to ensure good gripping. The preload was then reduced to .5 kN prior to the start of each test.

2.6.3 Digital Image Correlation (DIC)

DIC is an optical imaging method used to measure deformation on the surface of a specimen during testing. Cameras track the gray value pattern in small regions known as subsets, and the software correlates the relative motion of these subsets with the strain in various directions.

DIC was used during tensile testing to gain additional insight into the stress-strain behavior of the flake reinforced laminates. Each tensile specimen was spray painted white with black speckles to create a high contrast speckle pattern for the cameras to track. Correlated Solutions' Vic-3D 2010 software used for analysis.

2.7 Physical Characterization of the Laminates

2.7.1 Density

The densities of the laminates were determined using the Archimedes method described in ASTM D792 *(32)*. The densities were measured for at least 5 specimens per laminate. The densities of a cast epoxy sample, a cast vinyl ester sample, and a cured 10-ply unidirectional T800S/3900-2 laminate were determined as well so that the flake volume fractions could be determined from the following equation:

$$V_F = \frac{\rho_c - \rho_m}{\rho_F - \rho_m} \qquad \text{[Equation 9]}$$

where V_F is the volume fraction of the flakes, ρ_c is the density of the flake reinforced composite, ρ_F is the density of the flake (the density of the cured 10-ply T800S/3900-2 laminate), and ρ_m is the density of the matrix.

It was assumed that the density of the flakes was the same as the density of a cured 10-ply T800S/3900-2 laminate. The densities of the single ply flakes may have been slightly higher than the density of a laminate if a significant amount of resin infiltrated the peel ply during the cure cycle. For a thicker laminate with peel ply on the top and bottom surfaces, the amount of resin drawn away from the composite by the peel ply would be negligible. However, this may not be true for single plies with peel ply on both sides. It was also assumed that there was no porosity in

the laminates. If porosity is present in a laminate, then the calculated flake volume fraction will be lower than the actual fiber volume fraction because the measured density will be less than the density of a void free laminate but the volume percentage of the flakes will be the same.

The fiber volume fraction was determined by multiplying the flake volume fraction by the fiber volume fraction within a flake. The weight % of fibers in T800S/3900-2 resin is approximately 65%. The density of T800S fibers is 1.80 g/cc *(33)*, and the density of epoxy was estimated at 1.25 g/cc. Converting weight % to volume % yields a T800S/3900-2 fiber volume fraction of 56%. Therefore, each calculated flake volume fraction was multiplied by .56 to give an approximation of the fiber volume fraction of each flake reinforced laminate.

2.7.2 Optical Microscopy

Cross sections from each of the 25.4 cm by 25.4 cm (10 in by 10 in) laminates were imaged at a magnification of 5X with an Olympus BX51 microscope with attached Olympus SC30 digital camera to assess laminate quality and flake distribution. Images of the failure surfaces of the flexure and tension specimens were imaged at magnifications of 3.75 and 35X with an Olympus SZH10 stereo microscope with attached Tuscen TCC-5.0C digital camera. This was done to assess the failure characteristics of the laminates and to determine their failure modes in both flexure and tension.

Chapter 3: Results and Analysis

3.1 Results and Analysis Overview

The results of this research are presented in several parts based on the flake type within the laminates and the type of mechanical testing performed. Optical microscopy of the shredded and single ply flakes is presented first, followed by the preliminary flexure results from the 15.2 cm by 15.2 cm (6 in by 6 in) laminates. The results from the smaller laminates influenced the fabrication and testing of the larger 25.4 cm by 25.4 cm (10 in by 10 in) laminates. Hence, the results for the larger laminates are presented next. These results include the effect of flake geometry on the flexural and tensile properties of single ply flake/vinyl ester laminates, as well as analysis of the fracture surfaces of the flexure and tension specimens. Digital image correlation results for a single ply flake/vinyl ester tensile specimen are included as well. The mechanical properties of the single ply flake/vinyl ester laminates are compared to the properties of several other materials, including the shredded flake/vinyl ester laminate. Finally, a shear-lag model for flake reinforced laminates is discussed and the flexural moduli of the single ply flake laminates are compared to predictions based on the longitudinal and transverse rule of mixtures equations. Data scatter is discussed near the end of the chapter as well.

3.2 Optical Microscopy of the Flake Reinforcement

3.2.1 Shredded Flakes

Although the conditions and parameters of the shredding process were unspecified, shredding was found to cause significant microcracking in the flakes. This is shown below in Figure 9. The bottom image in the figure is the top image at a higher magnification.

Figure 9: Cracked shredded flake at two different magnifications

Cracks infused with pink mounting resin are clearly seen in the shredded flake shown above. This flake is representative of the many shredded flakes that were imaged and shows the typical

crack features observed. Most cracking was intralaminar; almost no regions of delamination were seen within a flake. This is likely due to the presence of interlayer toughener particles between plies. The top and bottom surfaces of the flakes show where the shredding process broke apart the original material both interlaminarly and intralaminarly. In Figure 9, the bottom surface of the flake pictured includes the resin-rich area and the interlayer toughener particles that exist between the plies. The top surface of this flake is much less uniform and was created where the recyclate cracked intralaminarly through a ply.

An interesting feature of Figure 9 is the large crack that runs left to right and bridges two plies. In general, most of the cracking was observed within the individual plies and often originated at the end of a flake and proceeded inwards, as seen in Figure 10 below.

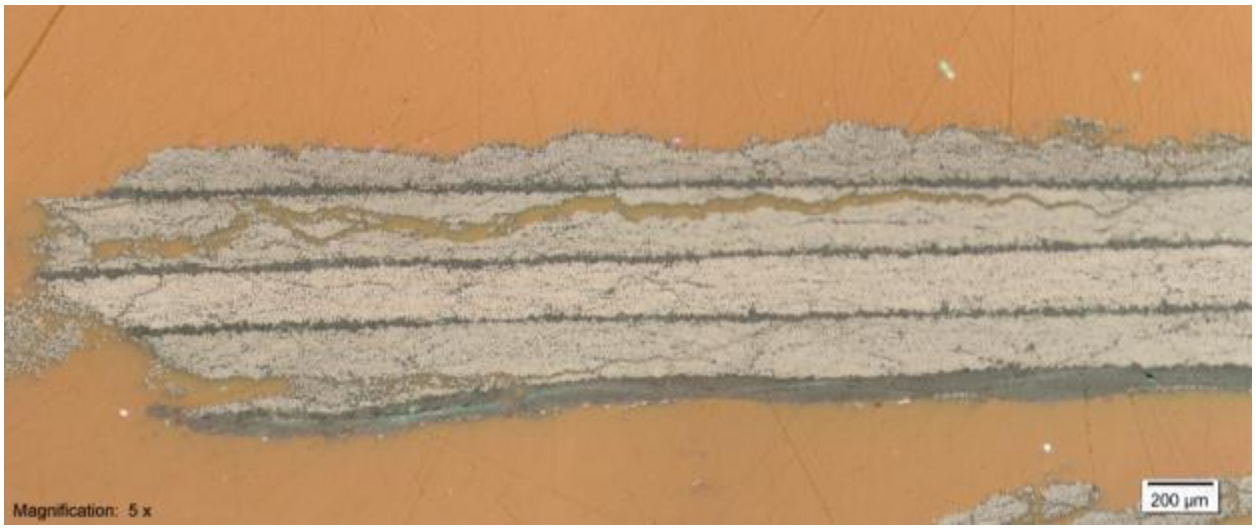

Figure 10: Cracked shredded flake

3.2.2 Single Ply Flakes

Figure 11 below shows several single ply flakes mounted in pink epoxy.

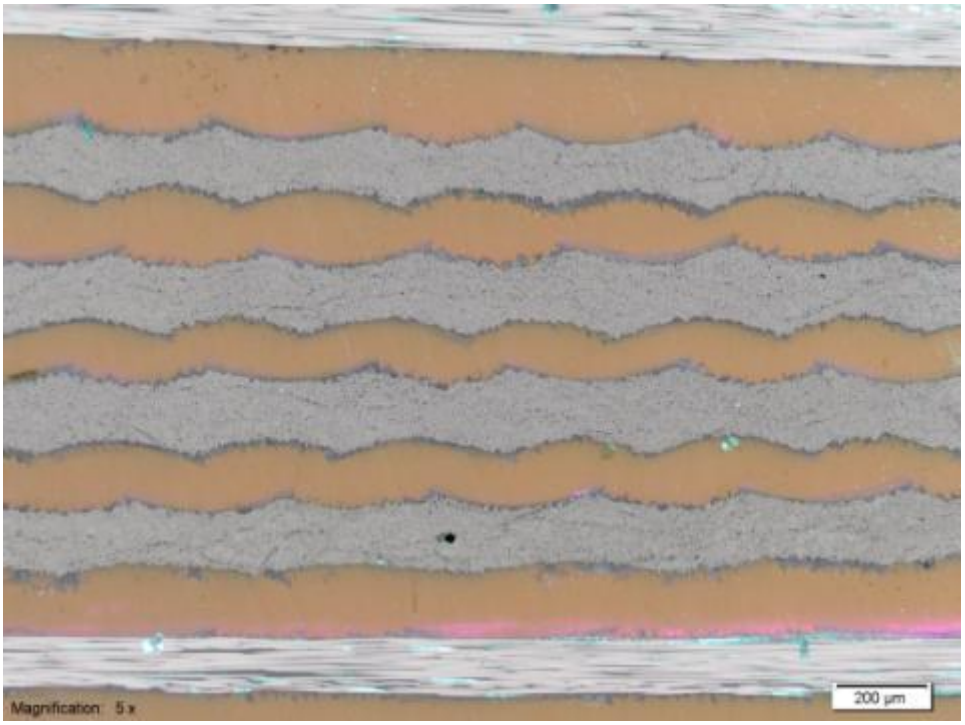

Figure 11: Single ply flakes

The texture from the peel ply is clearly evident in the four single ply flakes in the center of the image above. The waviness in the top and bottom surfaces was created by the plain weave of the peel ply. No cracks are seen in the flakes shown above. However, a flake with a longitudinal crack in the fiber direction is shown below in Figure 12.

Figure 12: A cracked single ply flake mounted between two uncracked single ply flakes

Although a cracked single ply flake is shown in Figure 12 above, very few cracked flakes were observed among the many that were imaged. Some cracking was expected during handling since the flakes were stored in plastic bags and moved several times. In an optimum laminate fabrication process, handling of the flakes could be significantly reduced and the flakes could be scattered in the mold immediately after they were cut.

Figure 12 above also shows the peel ply texture left on the surfaces of the single ply flakes. The imprint left by the individual peel ply fibers is visible in addition to the coarse waviness created by the plain weave of the peel ply. This fine texture is best illustrated in Figure 13 below.

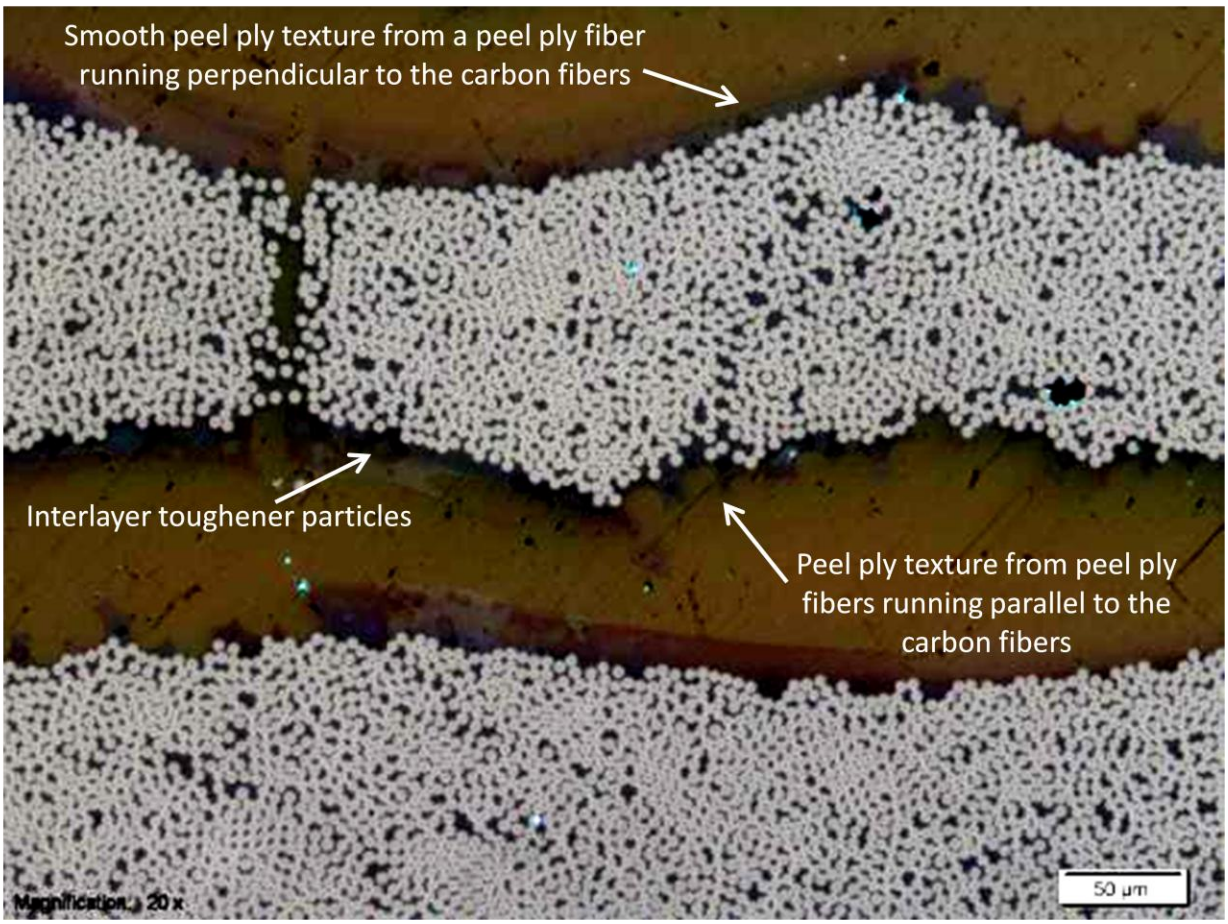

Figure 13: Single ply flakes with evident peel ply texture

Figure 13 shows two single ply flakes mounted in pink epoxy. The fine texture created in the surfaces of single ply flakes when the peel ply is removed is clearly evident. When the peel ply is removed, cylindrical channels are left in the matrix resin on the surface of the flakes where the peel ply fibers were embedded. In Figure 13, circular cross sections of the channels on the flake surfaces left from peel ply fibers oriented parallel to the carbon fibers in the flakes are seen filled in with the pink mounting epoxy. Fibers from peel ply tows oriented perpendicular to the fibers also left channels that appear in Figure 13 as a long smooth flake surface since only one channel can be seen. Although the peel ply removes some of the surface epoxy, some interlayer toughener particles are also visible on the surfaces of the flakes. These particles are added to both surfaces of T800S/3900-2 prepreg during manufacturing and are meant to increase the toughness and delamination resistance of laminated composites.

3.3 The Effect of Matrix Resin Type on the Flexural Properties of Flake Reinforced Laminates

Figures 14 and 15 below show the difference in flexural properties for 15.2 cm by 15.2 cm (6 in by 6 in) laminates fabricated with either 1.27 cm by 1.27 cm (.5 in by .5 in) single ply flakes or shredded flakes and either epoxy or vinyl ester resin.

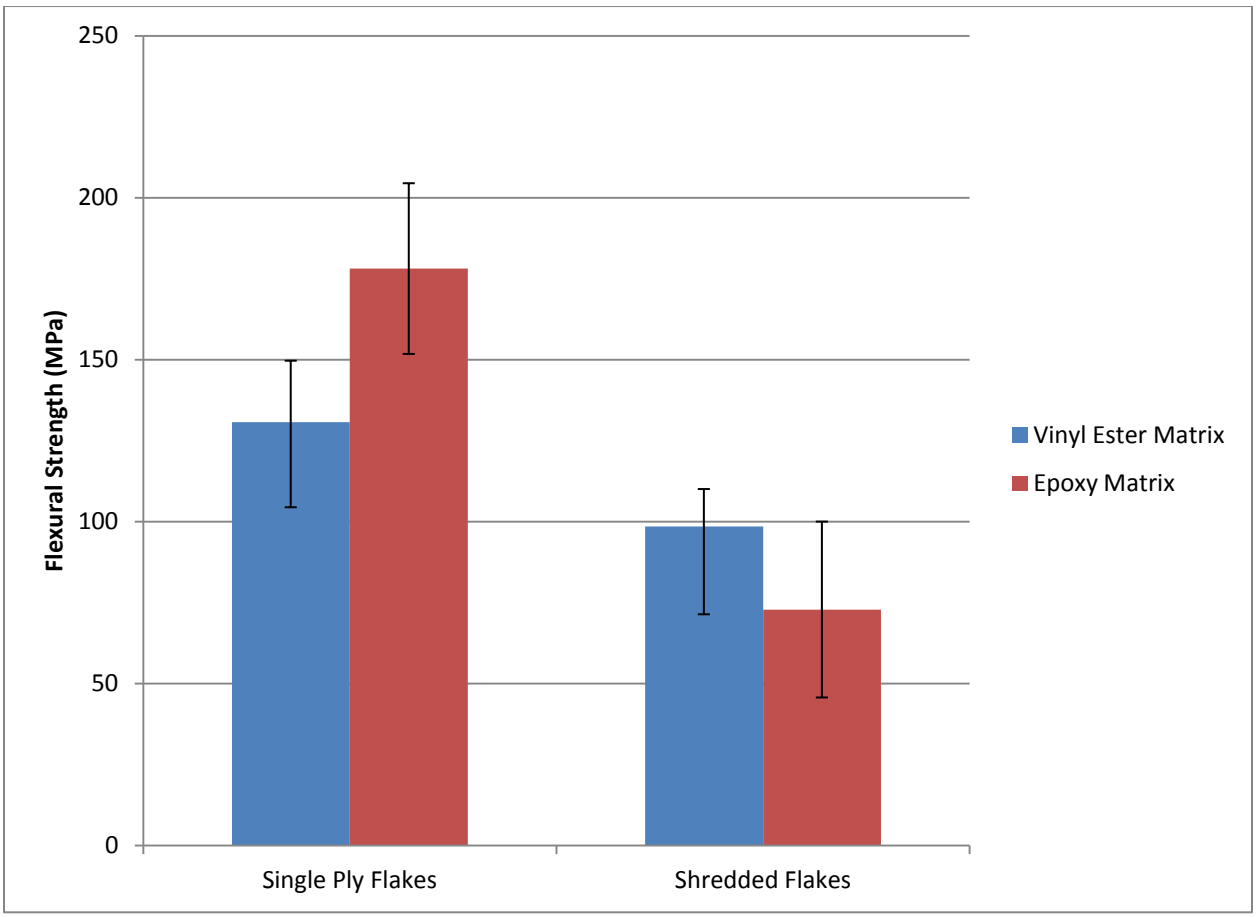

Figure 14: The effect of matrix resin type on the flexural strength of flake reinforced laminates

Figure 14 above shows opposing trends in the flexural strength of laminates fabricated with either single ply flakes or shredded flakes and either epoxy or vinyl ester resin. The flexural strength of the single ply flake/vinyl ester laminate was lower than that of the single ply flake/epoxy laminate, while the flexural strength of the shredded flake/vinyl ester laminate was higher than that of the shredded flake/epoxy laminate. However, when the scatter in the data is

considered and the magnitudes of the error bars are evaluated, each of these trends is much less apparent. It should be noted that all the error bars included in the charts in this chapter represent the standard deviation of the relevant data set.

The error bars for the flexural strengths of the shredded flake/epoxy and shredded flake/vinyl ester laminates overlap significantly. Some scatter is expected in flexural strength data because the load is being concentrated in one location during the three point bend test and the strength of the material is typically controlled by the largest defect in the material. Specimens with defects located where the stress is concentrated will have lower strengths than laminates that do not have defects in these locations.

Figure 15 below shows the effect of matrix resin type on the flexural moduli of laminates fabricated with either single ply flakes or shredded flakes and either epoxy or vinyl ester resin.

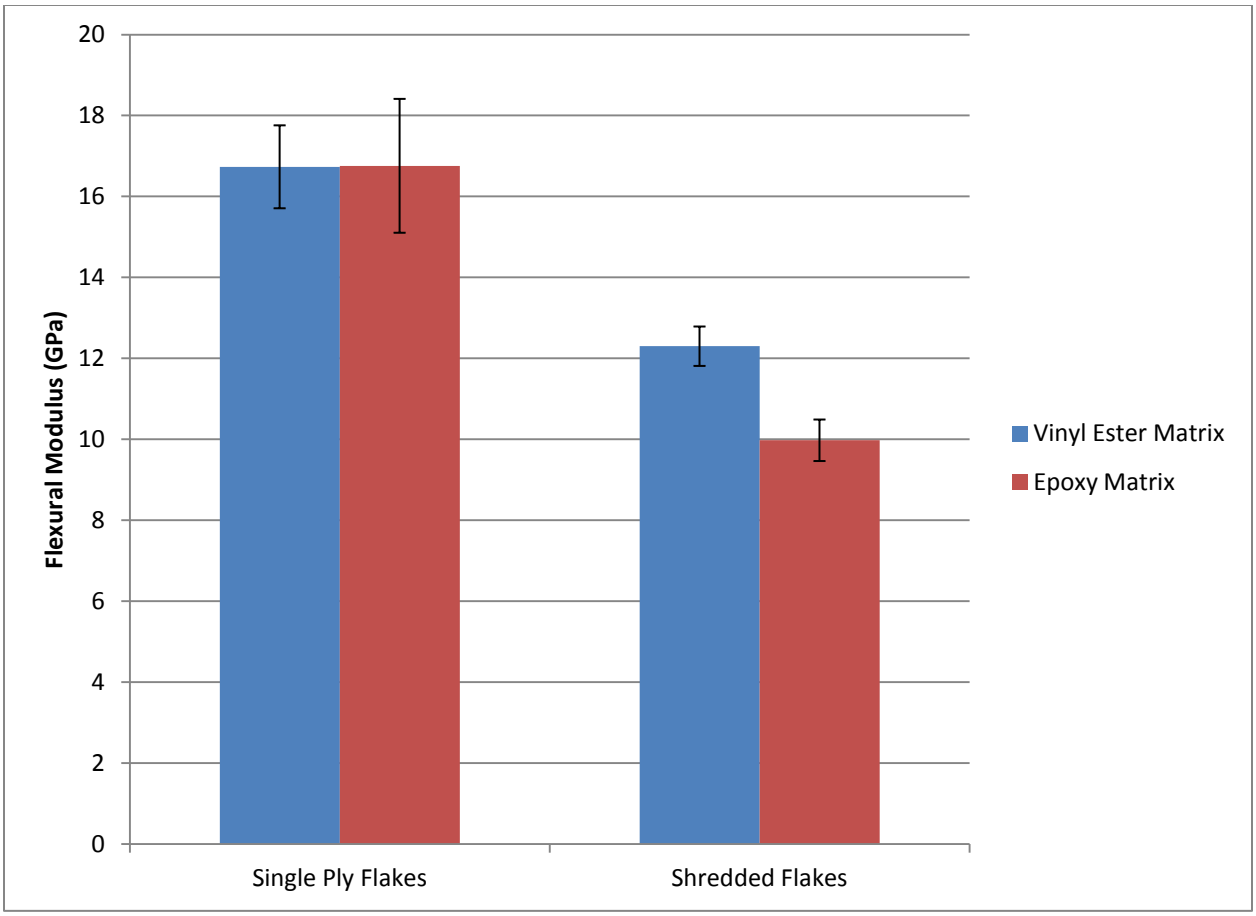

Figure 15: The effect of matrix resin type on the flexural modulus of flake reinforced laminates

As seen in Figure 15, there is almost no difference in the flexural moduli of single ply flake/epoxy and single ply flake/vinyl ester laminates. The average flexural modulus of each of the two laminates is nearly identical, and the error bars are similar as well. The trend in flexural modulus observed for the shredded flake/epoxy and shredded flake/vinyl ester laminates is the same as that observed for flexural strength. However, the error bars are much smaller and do not overlap as they did in Figure 14. Smaller scatter in flexural modulus data is expected since the modulus should only depend on bonding and flake volume fraction. Some scatter in all the mechanical properties of the flake reinforced laminates is expected due to inherent variations in flake volume fraction and the degree of flake randomness throughout the volume of the laminates, as will be discussed in section 3.5. Overall, the volume fractions of all the single ply flake laminates should be nearly identical since the same weight of flakes was used in each laminate and the flakes were all of the same geometry. The same weight of flakes was used to

fabricate each of the two shredded flake laminates as well. However, the high geometric variation in the shredded flakes may inhibit good packing and result in large regions of high resin content and thus low flake volume fractions. As long as a large enough area is considered, the flake volume fractions of the two shredded flake laminates should be the same.

Since there were no significant differences in the flexural properties of flake reinforced/epoxy and flake reinforced/vinyl ester laminates, vinyl ester was chosen as the matrix resin for the 25.4 cm by 25.4 cm (10 in by 10 in) laminates. This resin type was preferred over epoxy because its lower viscosity eliminated the need for degassing prior to infusion and contributed to faster infusion times.

3.4 The Effect of Fines on the Flexural Properties of Shredded Flake Reinforced Laminates

Figures 16 and 17 below show the differences in the flexural properties of shredded flake/epoxy and shredded flake/vinyl ester laminates with and without the fines removed by washing the shredded flakes in acetone prior to resin infusion.

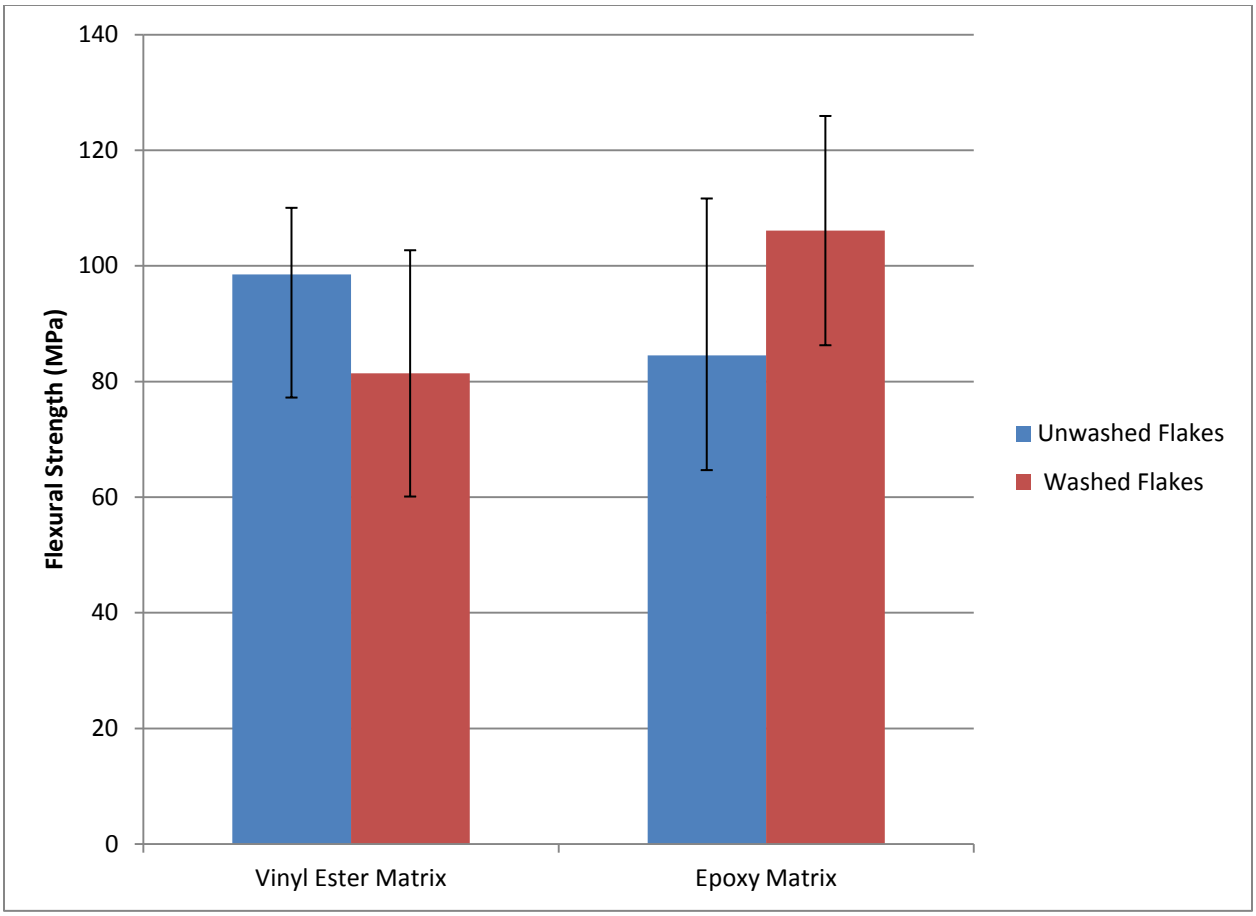

Figure 16: The effect of fines on the flexural strength of shredded flake reinforced laminates

As seen in Figure 16, the flexural strength of the shredded flake/vinyl ester laminate with unwashed flakes was higher than that of the shredded flake/vinyl ester laminate with washed flakes. This was the opposite trend observed for the shredded flake/epoxy laminates with washed and unwashed flakes. Again, the error bars are quite large. Washing the flakes may have had a small effect on the flexural strength of the shredded flake reinforced laminates, but this effect may have been masked by the large scatter in the data.

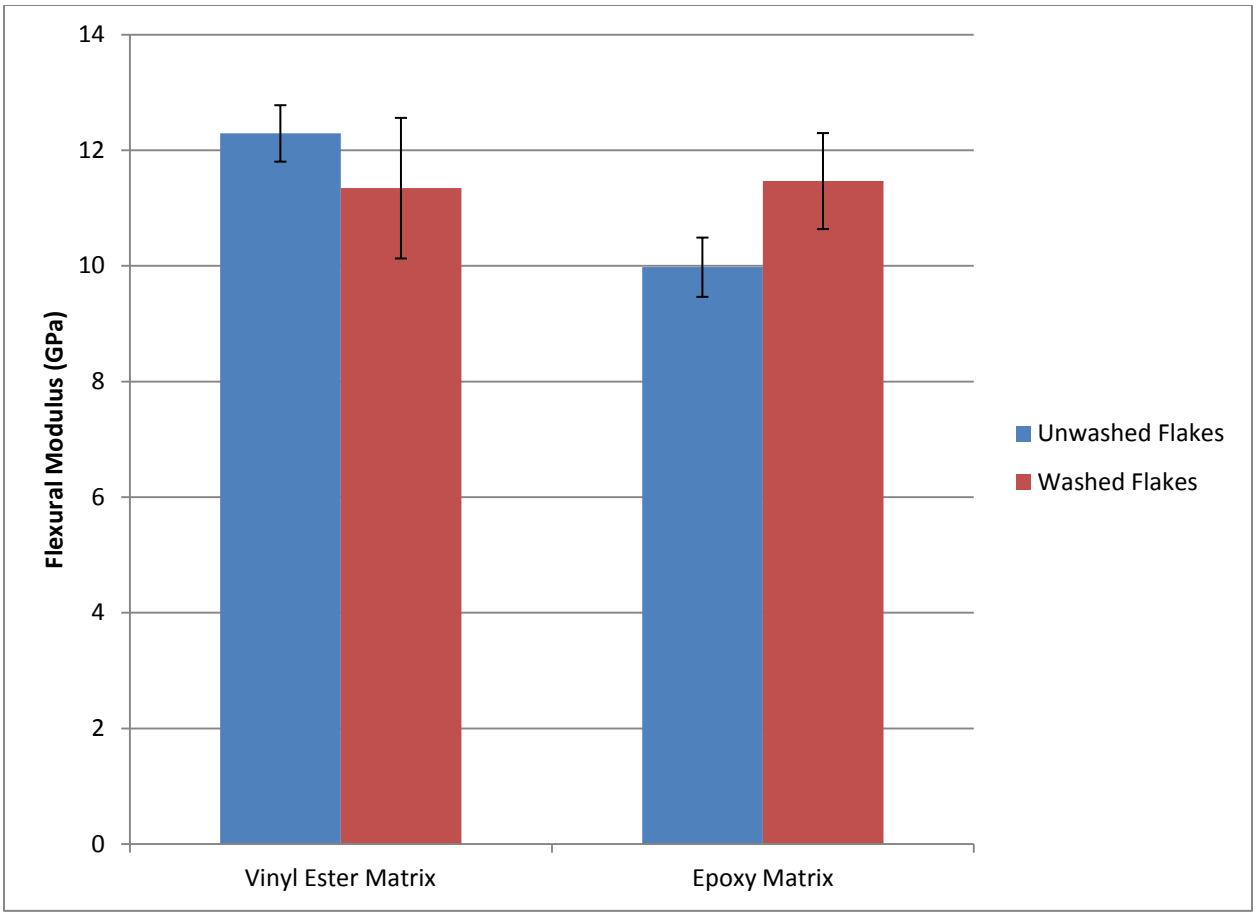

Figure 17: The effect of fines on the flexural modulus of shredded flake reinforced laminates

As with flexural strength, the flexural modulus of the shredded flake/vinyl ester laminate fabricated with washed flakes was lower than that of the shredded flake/vinyl ester laminate fabricated with unwashed flakes. This was the opposite trend observed for the shredded flake/epoxy laminates with washed and unwashed flakes. However, when error bars are evaluated, there is no significant difference in the flexural strength or the flexural modulus of washed and unwashed shredded flake reinforced laminates. The shredded flakes for the 25.4 cm by 25.4 cm (10 in by 10 in) laminates were therefore not washed.

3.5 Physical Characterization of the 25.4 cm by 25.4 cm (10 in by 10 in) Laminates

The flake and fiber volume fractions of each of the 25.4 cm by 25.4 cm (10 in by 10 in) laminates are given in Table 2 below. Although the density of at least five specimens was

measured for each laminate, it should be noted that these specimens came from only one side of each laminate.

Table 2: Physical characteristics of the 25.4 cm by 25.4 cm (10 in by 10 in) laminates

Flake Type	Flake Size (cm by cm)	Flake Size (in by in)	Flake Aspect Ratio	Flake Area (cm^2)	Flake Area (in^2)	Density (g/cc)	Flake Volume Fraction	Fiber Volume Fraction
Single Ply	1.27 x 1.27	.5 x .5	1:1	1.61	.25	1.32	0.43	0.24
Single Ply	2.54 x .64	1 x .25	4:1	1.61	.25	1.33	0.44	0.25
Single Ply	1.78 x .89	.7 x .35	2:1	1.61	.25	1.34	0.47	0.26
Single Ply	2.54 x 1.27	1 x .5	2:1	3.23	.5	1.35	0.48	0.27
Single Ply	2.54 x 2.54	1 x 1	1:1	6.45	1	1.37	0.53	0.30
Shredded Flake	N/A	N/A	N/A	N/A	N/A	1.30	0.37	0.21

In general, the fiber volume fractions of the laminates are relatively low. Most recycled laminates have a fiber volume fraction near 30%. The highest achieved fiber volume fraction found in the literature for a recycled CFRP composite was 40% *(3)*. Although one of our laminates did have a fiber volume fraction of 30%, the average fiber volume fraction was 26.4%. In order to achieve a fiber volume fraction of 40%, we would need to have a flake volume fraction of 71%.

Since all the laminates were fabricated via the same method with the same weight of flakes, all of the laminate densities (and thus all of the calculated flake and fiber volume fractions) were expected to be similar. As seen in Table 2, each of these properties increased with increasing flake size, but only by a small amount. The maximum difference in densities among two laminates was 3.8%. The differences are larger for the calculated flake and volume fractions because the equations for these properties depend on density.

Larger area flakes may have higher densities and flake and fiber volume fractions because of better flake packing and fewer low-density resin pockets between flakes. Figure 18 below shows two typical cross sections for each laminate. Each image on the left is a representative image of

the highest flake packing in a laminate, while each image the right is a representative image of the lowest flake packing in that same laminate. All images were taken at an original magnification of 5X. From top to bottom, the flake size in each laminate follows the order listed in Table 2. Each set of images is labeled with the flake size as well. This top-to-bottom order remains the same in subsequent figures that compare the characteristics of the 25.4 cm by 25.4 cm (10 in by 10 in) single ply flake laminates.

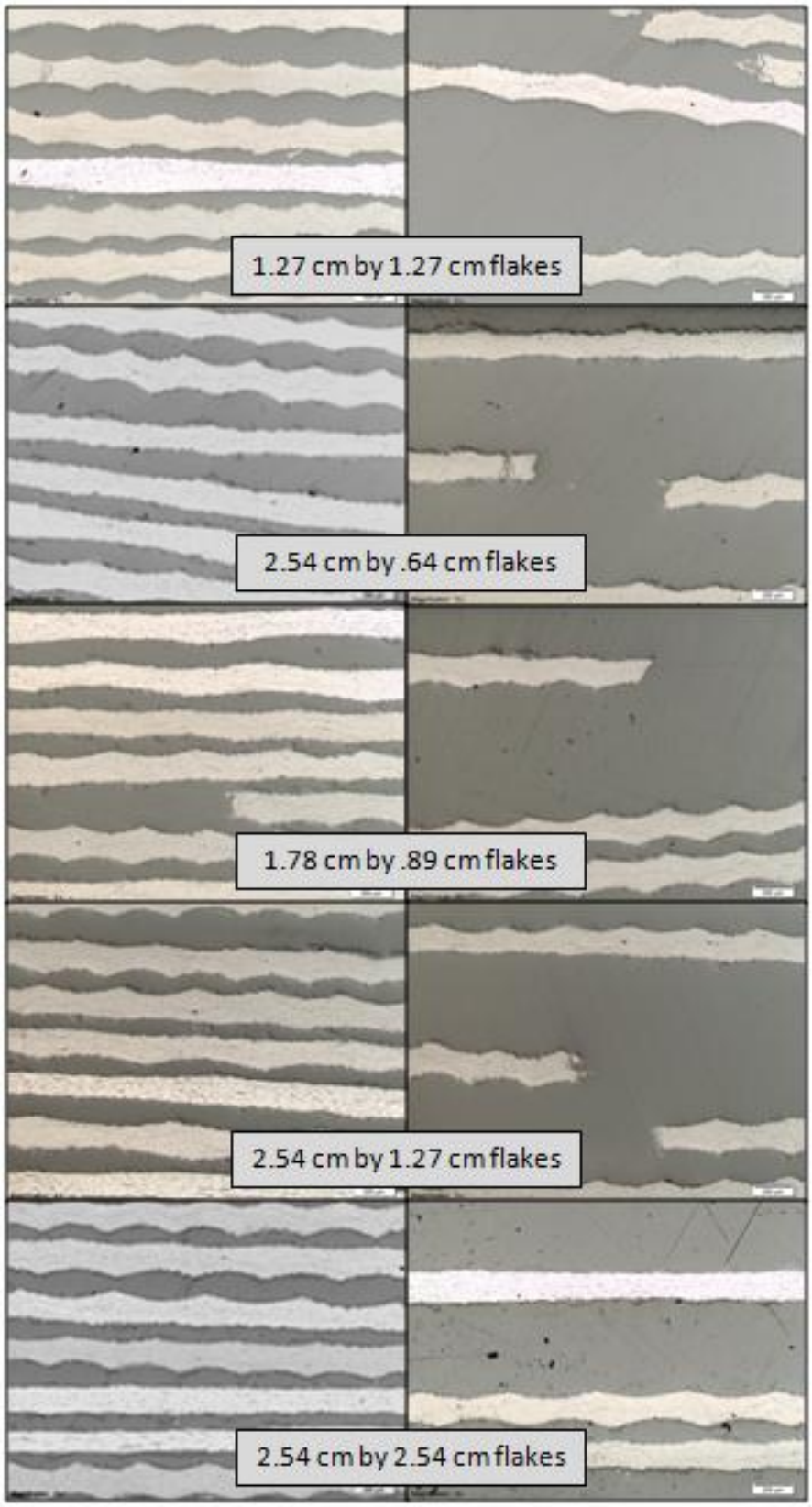

Figure 18: Regions of high and low flake packing in single ply flake/vinyl ester laminates

As seen in Figure 18, all of the single ply flake/vinyl ester laminates had comparable regions of high and low flake packing. However, it is possible that the laminates with higher volume fractions had fewer regions of low flake packing. Improved fiber volume fractions, and thus improved mechanical properties, could be achieved by eliminating the resin pockets seen in Figure 18, improving the uniformity of flake distribution, and increasing the flake packing density. This may require curing the laminates under pressure after the preforms are infused but before the resin has gelled, or using an alternative fabrication process such as compression molding. An automated process for scattering the flakes in the mold would also likely improve the uniformity of flake distribution as well as the degree of randomness of the scattered flakes. We assumed that randomly scattering the flakes by hand would result in a completely random flake orientation. However, this was not verified.

Disparities in the densities, flake volume fractions, and fiber volume fractions among different single ply flake/vinyl ester laminates may also be partially attributed to porosity. A specimen with high porosity would have a lower density than a specimen with no porosity, but the same volume percentage of fibers. This would result in a calculated flake volume fraction that is lower than the actual flake volume fraction. The single ply flake/vinyl ester laminates fabricated with 1.78 cm by .89 cm (.7 in by .35 in) flakes and 2.54 cm by .64 cm (1 in by .25 in) flakes had visible porosity and were among the laminates with the lowest calculated flake volume fractions. Porosity in the single ply flake/vinyl ester laminates fabricated with 2.54 cm by .64 cm (1 in by .25 in) flakes is shown below in Figure 19.

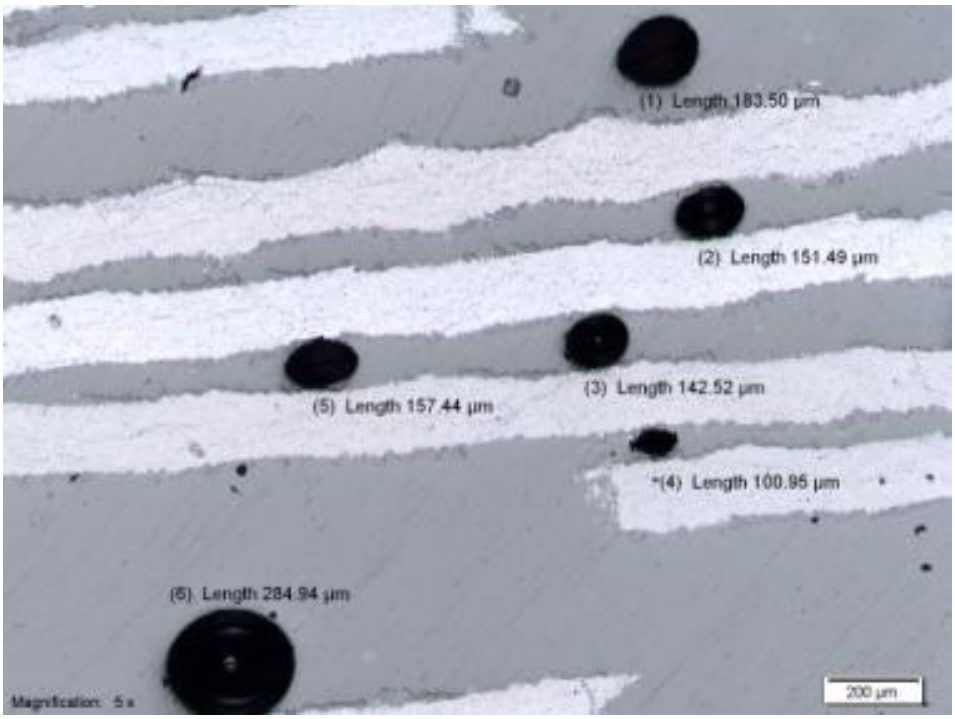

Figure 19: Single ply flake/vinyl ester laminate with significant porosity

Figure 19 above shows significant porosity in a single ply flake/vinyl ester laminate. The average size of the voids was approximately 170 µm. The largest void in the 2.54 cm by .64 cm (1 in by .25 in) cross section imaged was 787 µm. Porosity in the laminates was likely to due improper VARTM conditions. During infusion, bubbles were seen to form in the resin where the inlet tube was pinched by clamp regulating resin flow. While the vacuum was expected to remove these bubbles, it is possible that the bubbles could not be removed effectively in all cases, or that the resin gelled before the bubbles were fully removed. Laminate quality also may have been higher if we had used the controlled atmospheric pressure resin infusion (CAPRI) process to infuse the laminates instead of VARTM. Higher quality laminates can be fabricated with CAPRI because the pressure differential between the inlet and the outlet can be controlled and the outlet side does not remain at atmospheric pressure as it does with VARTM.

In many of the subsequent charts in this chapter, specific properties are plotted along with nominal values to account for minor differences in flake volume fractions. However, the observed trends are essentially the same regardless of whether nominal or specific properties of the different laminates are considered. The density differences among the laminates were

relatively small, but small differences in density can be indicative of substantially different flake or fiber volume fractions. Hence, both nominal and specific properties were included.

3.6 The Effect of Flake Geometry on the Flexural Properties of Single Ply Flake/Vinyl Ester Laminates

Figure 20 below shows the flexural strengths of the single ply flake/vinyl ester laminates fabricated with flakes of different geometries. The chart is separated into two sections based on flake geometry. The left side of the chart shows how flexural strength varies with increasing aspect ratio for a constant flake area of 1.61 cm^2 (.25 in^2), while the right side of the chart shows how flexural strength varies with increasing aspect ratio for a constant flake length of 2.54 cm (1 in). For each data set, the flake length and width are listed first, followed by the flake aspect ratio in parenthesis. It should be noted that the data for the single ply flake/vinyl ester laminate fabricated with 2.54 cm by .64 cm (1 in by .25 in) flakes was plotted twice-once for the constant flake area data set and once for the constant flake length data set. The organization of Figures 21, 23, and 24 are the same as that of Figure 20.

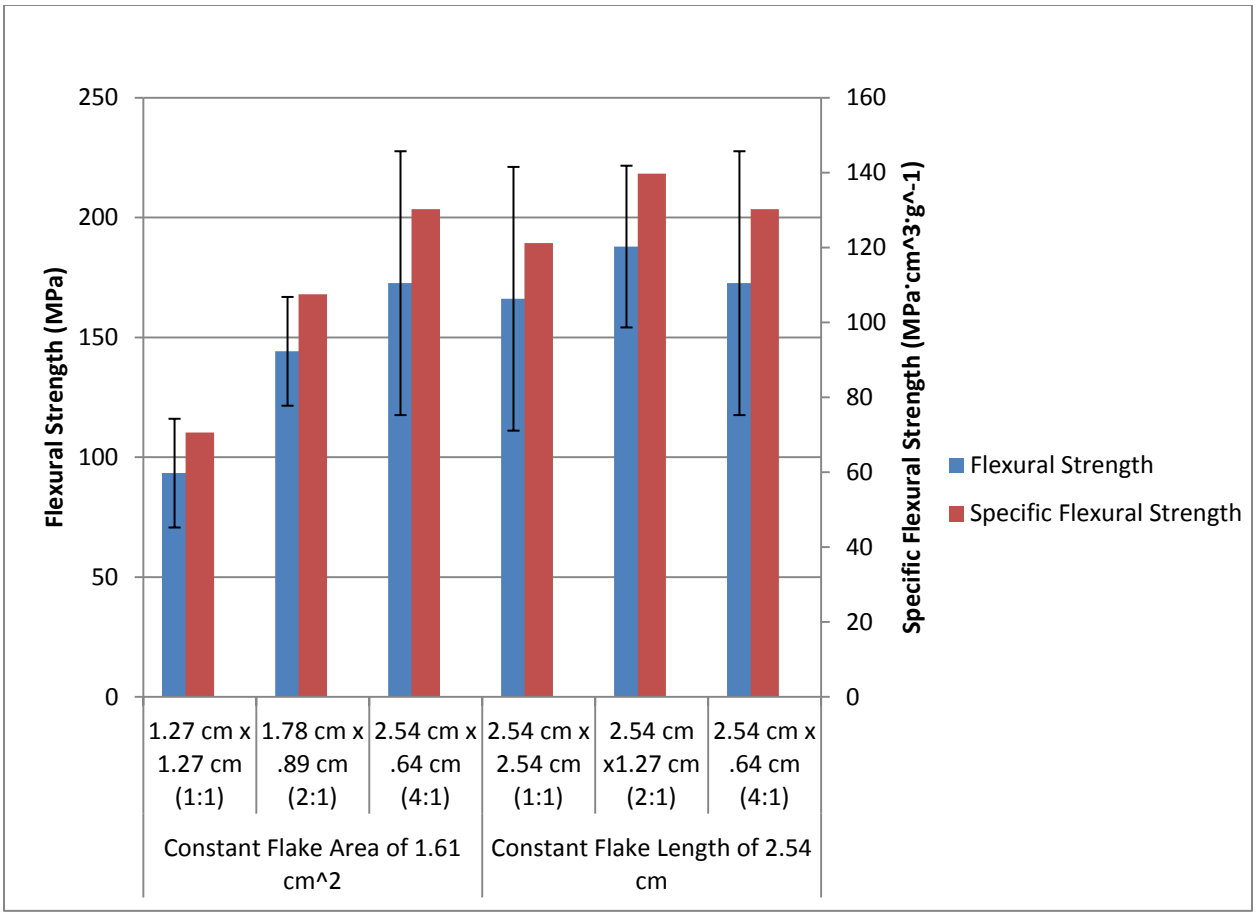

Figure 20: The effect of flake geometry on the flexural strength of single ply flake/vinyl ester laminates

As seen in Figure 20, flake length has more of an effect on flexural strength than either flake area or flake aspect ratio. This trend is evident despite the relatively large error bars shown. Flexural strength increases with increasing aspect ratio for a constant flake area, but flake length is increasing in this data set as well. Flexural strength is relatively constant among all the 2.54 cm (1 in) long flakes, regardless of width or aspect ratio. This trend is less evident for the flexural moduli of single ply flake/vinyl ester laminates fabricated with flakes of different geometries, as seen below in Figure 21.

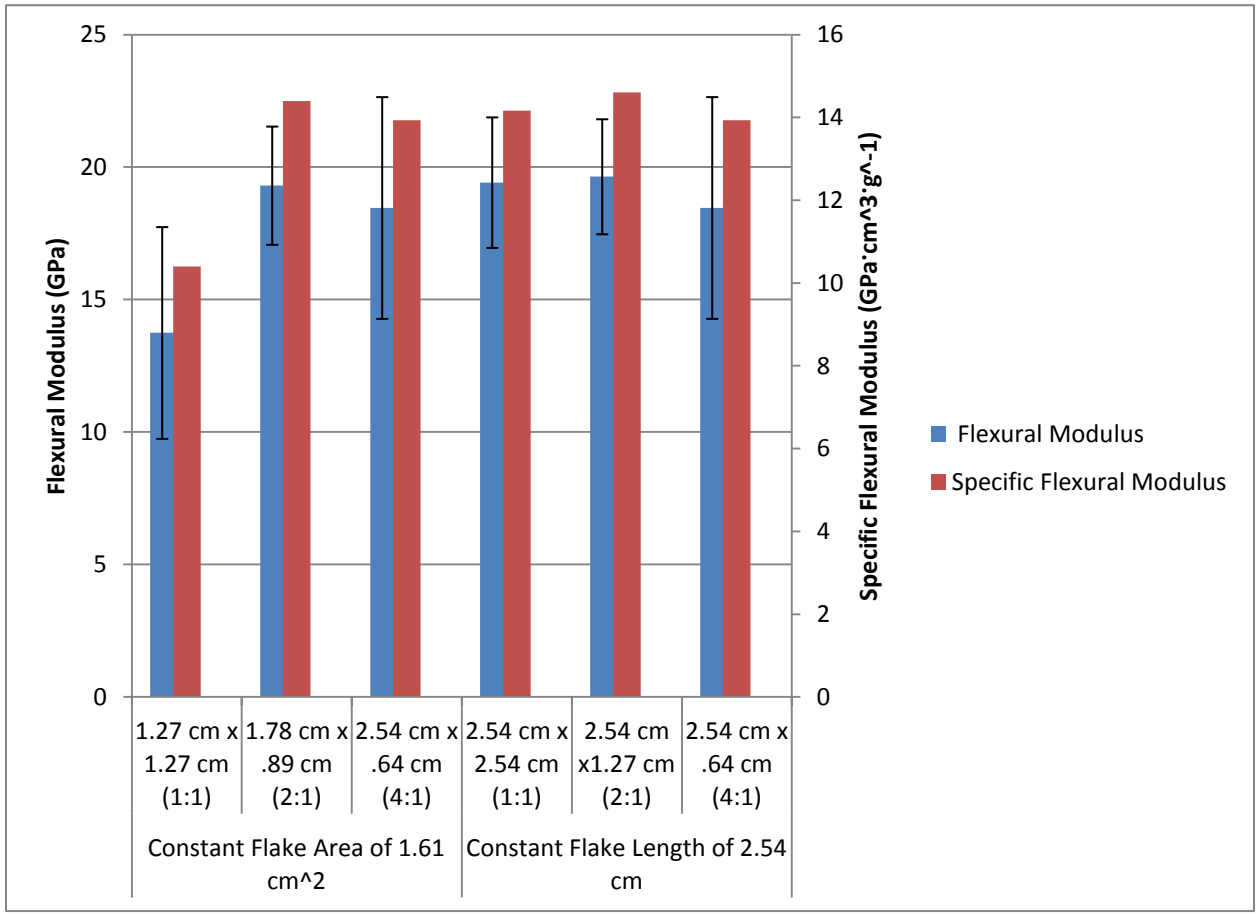

Figure 21: The effect of flake geometry on the flexural modulus of single ply flake/vinyl ester laminates

As seen in Figure 21, the flexural modulus is relatively consistent among all the laminates except for the single ply flake/vinyl ester laminate fabricated with 1.27 cm by 1.27 cm (.5 in by .5 in) flakes.

3.7 Flexural Failure Modes of Single Ply Flake/Vinyl Ester Laminates

Analysis of the fracture surfaces of the single ply flake-vinyl ester specimens tested in flexure shows poor bonding between the flakes and the vinyl ester. Figure 22 below shows representative fracture surfaces of a flexure specimen from each of the single ply flake/vinyl ester laminates fabricated with flakes of different geometries. Each specimen was broken completely in half by manual control of the load frame after the initial failure occurred and

testing had automatically stopped. All images in Figure 22 were taken at an original magnification of 3.75X.

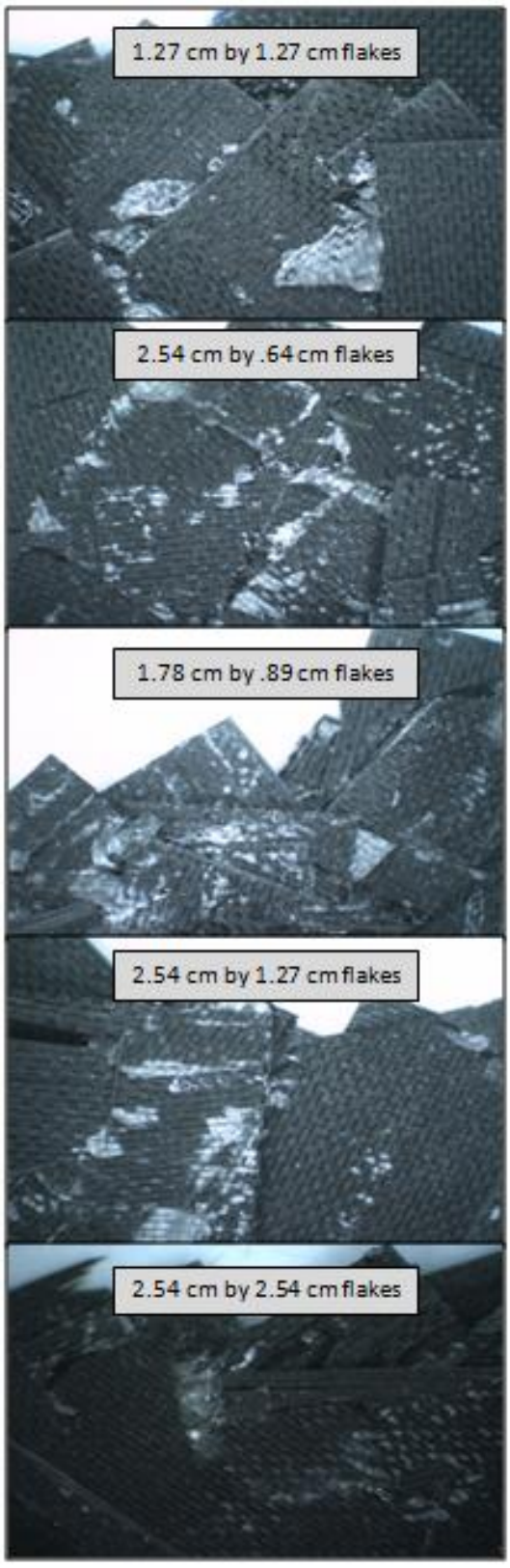

Figure 22: Fracture surfaces of single ply flake/vinyl ester flexure specimens

The peel ply texture can be seen on every exposed flake of every specimen shown above in Figure 22, as well as in some of the fragments of resin present on the fracture surfaces. This is because the resin conformed to the imprint of the peel ply on the surfaces of the flakes, but did not bond well to the surface. Failure occurred at the flake-matrix interface. Thus, disbonding was the dominant failure mode. The peel ply texture would not be visible if a good bond formed between the fiber and the matrix.

During testing, cracks were seen to grow around the edges of the flakes, rather than through them. A tortuous crack pathway that inhibits transverse crack growth would typically be desirable. However, the matrix must be well-bonded to reinforcement and should have relatively high toughness as well.

3.8 The Effect of Flake Geometry on the Tensile Properties of Single Ply Flake/Vinyl Ester Laminates

Figure 23 below shows the tensile strengths of the single ply flake/vinyl ester laminates fabricated with flakes of different geometries.

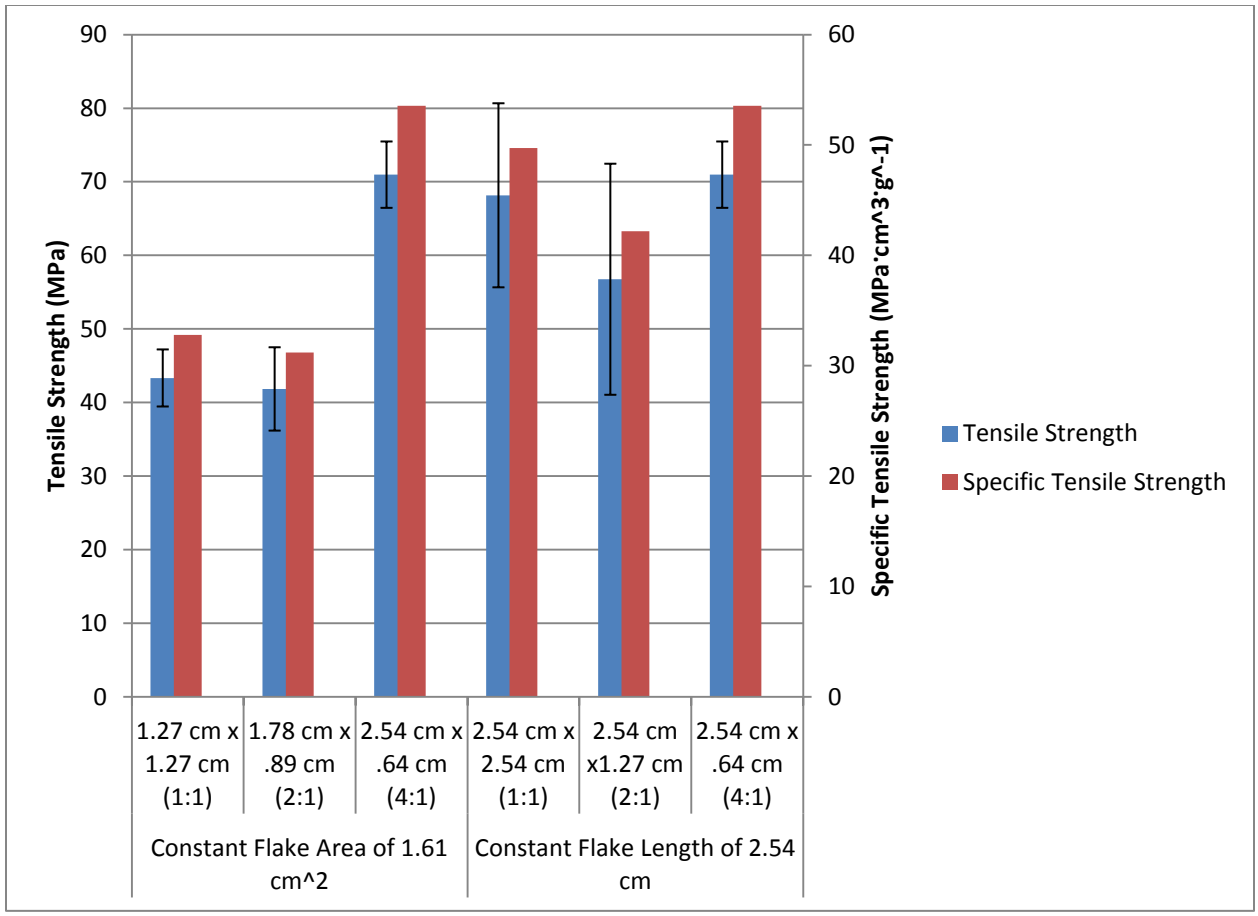

Figure 23: The effect of flake geometry on the tensile strength of single ply flake/vinyl ester laminates

As with flexural strength, tensile strength was greatest for the laminates with 2.54 cm (1 in) long flakes. Tensile strength did not show an increase with increasing aspect ratio and constant flake area until the aspect ratio became 4:1 and the flakes were 2.54 cm (1 in) long. Tensile strength was relatively constant for laminates with 2.54 cm (1 in) long flakes, regardless of aspect ratio. For the laminates with flake aspect ratios of either 1:1 or 2:1, the tensile strength was higher for laminates with longer flakes of the same aspect ratio. The tensile strength of the single ply flake/vinyl ester laminates fabricated with 2.54 cm by 1.27 cm (1 in by .5 in) flakes had a lower tensile strength than laminates with higher and lower aspect ratios but the same flake length. However, all the error bars for the laminates fabricated with 2.54 cm (1 in) long flakes overlap.

The trends observed for the average tensile strengths also hold true when the maximum measured tensile strength is analyzed, as shown below in Figure 24. The maximum tensile

strength for each laminate was taken as the maximum value of the strengths of the 5 specimens tested per laminate. Tensile strength is controlled by the largest flaw in the specimen. Therefore, analyzing the maximum tensile strength instead of the average tensile strength provides insight into the most optimally processed specimen (or the highest quality region of the laminate it came from).

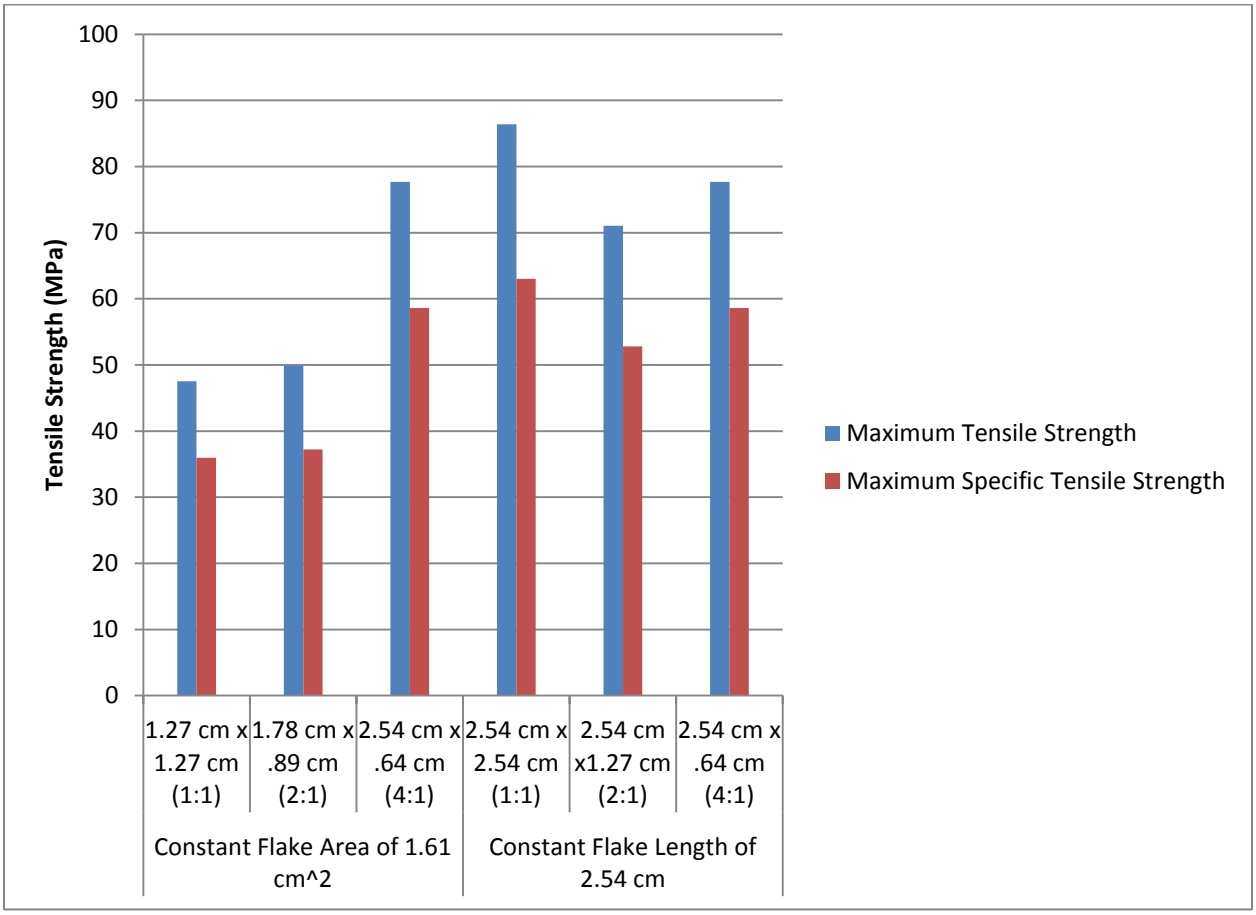

Figure 24: The effect of flake geometry on the maximum measured tensile strength of single ply flake/vinyl ester laminates

As seen in Figure 24, the trends observed for the average tensile strength also hold true for the maximum tensile strength. This result offsets the large error bars seen in Figure 22. Although there is a large amount of scatter in the data, the data averaged for a set of specimens is in agreement with the maximum values of the data and thus the highest quality regions of the

laminates produced. As with the average tensile strength, the maximum tensile strength of the single ply flake/vinyl ester laminate fabricated with 2.54 cm by 1.27 cm (1 in by .5 in) flakes is lower than the maximum tensile strength of laminates with higher and lower aspect ratios but the same flake length. This result indicates that laminate processing is not optimal. An increasing, decreasing, or constant trend was expected for flakes with increasing aspect ratios but the same flake length. Since there is no observable trend, it is likely that the single ply flake/vinyl ester laminates fabricated with 2.54 cm by 1.27 cm (1 in by .5 in) flakes had larger than average flaws that resulted in a relatively low tensile strength. The average and maximum tensile strength of this laminate were still significantly higher than the respective strengths of the laminates with shorter flake lengths.

Since crosshead displacement data is typically unreliable for obtaining accurate values of the tensile modulus, we intended to use the strain data from digital image correlation to determine this property for each of the laminates. The strain data obtained from digital image correlation is expected to be very accurate since strain can be averaged in any direction and over any desired region of the laminate as long as at least two cameras are used. Unfortunately, inexperience with the digital image correlation process and software led to experimental errors and prevented us from obtaining strain data for all the specimens. Some of these errors included improper image calibration, speckle patterns that were less dense than an ideal pattern, speckles that were too large, the use of a white paint that cracked on the surface when subjected to low strain levels, the use of tensile grips that obstructed the camera's view of the ends of the specimens, and inadvertent or unnoticed movement of the cameras that may have required re-calibration. Despite these errors, good data was obtained for some specimens. The digital image correlation software includes indicators during analysis that allow the user to determine if the data obtained is accurate, in agreement with the original calibration, and does not include significant noise. Hence, we are confident that the data presented below is accurate.

Figure 25 below shows a stress-strain curve generated by correlating the load recorded by the load frame software with the strain data obtained during digital image correlation of specimen B from the single ply flake/vinyl ester laminate fabricated with 1.27 cm by 1.27 cm (.5 in by .5 in) flakes.

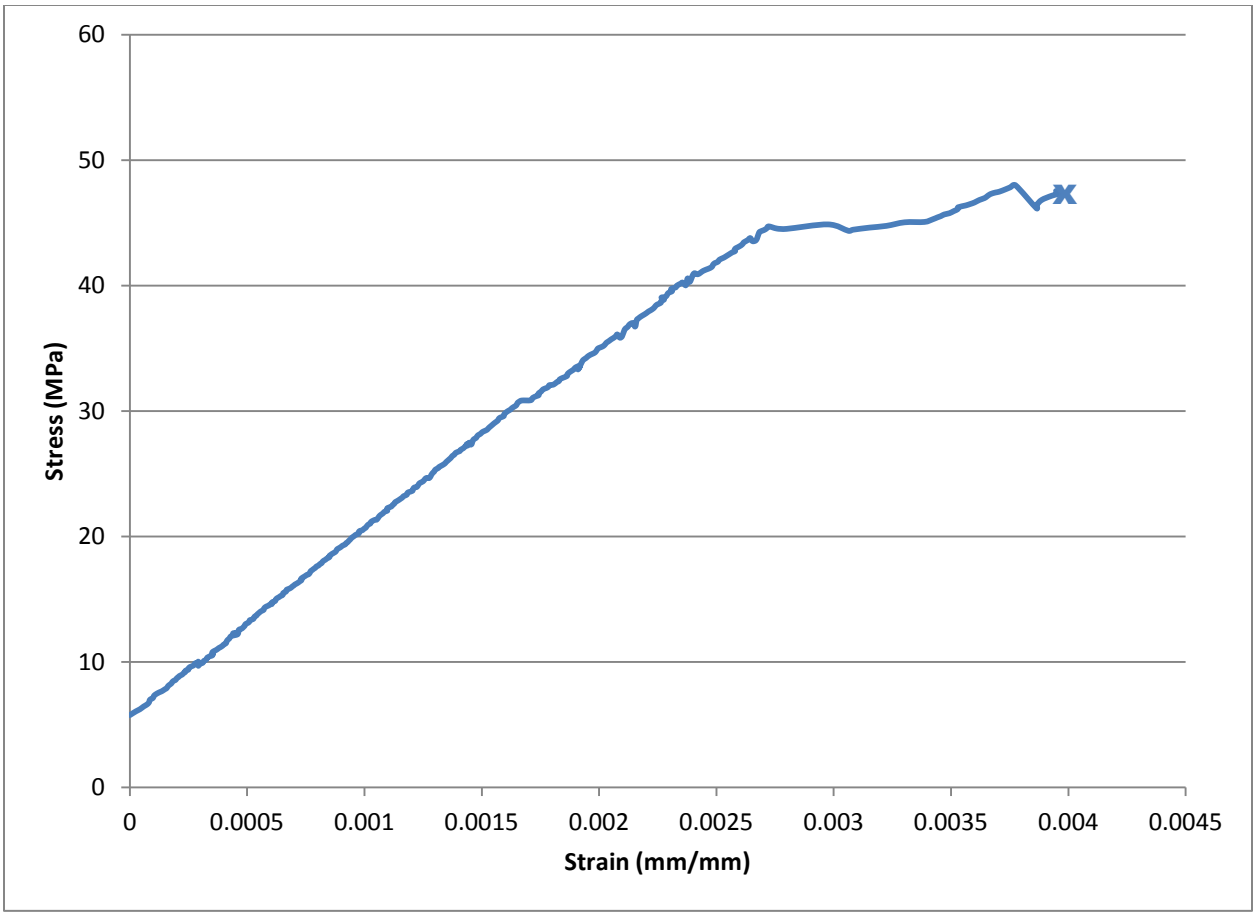

Figure 25: Stress-strain curve for one single ply flake/vinyl ester tensile specimen

As seen in Figure 25, the stress-strain behavior of the laminate is in accordance with what would be expected for a fiber reinforced laminate, but with more small fracture events and sustained damage before ultimate failure. The small, quickly recovered decreases in stress with increasing strain seen in the above plot correspond to matrix cracking in the laminate. Cracking was heard throughout the duration of each tensile test.

The tensile modulus of specimen B from the single ply flake/vinyl ester laminate fabricated with 1.27 cm by 1.27 cm (.5 in by .5 in) flakes as calculated from the above stress versus strain plot was 15.0 GPa. Since the flexural moduli of the single ply flake/vinyl ester laminates were relatively consistent, it can be assumed that all of the single ply flake/vinyl ester laminates would be also be approximately 15.0 GPa. This may be an underestimate of the tensile modulus of most of the laminates since the single ply flake/vinyl ester laminate fabricated with 1.27 cm by 1.27

cm (.5 in by .5 in) had the lowest flexural modulus of all the single ply flake/vinyl ester laminates.

3.9 Strain Evolution during Tensile Testing of a Single Ply Flake/Vinyl Ester Laminate

Figure 26 below shows axial strain contours plots generated with the digital image correlation during tensile testing of specimen B from the single ply flake/vinyl ester laminate fabricated with 1.27 cm by 1.27 cm (.5 in by .5 in) flakes. The evolution of the strain during testing is shown from left to right. It should be noted that areas shown in Figure 26 are approximately 2.54 cm wide by 7.62 cm long (1 in by 3 in).

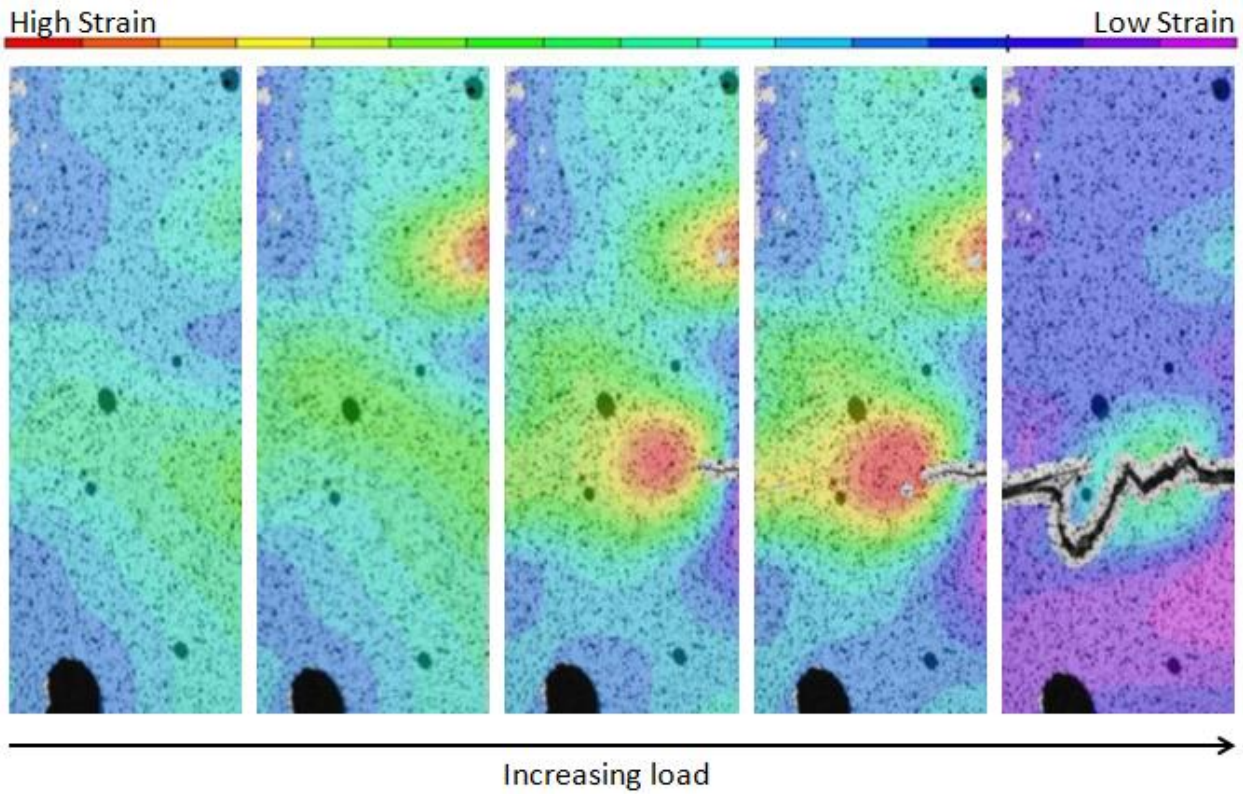

Figure 26: Axial strain evolution up to final failure in a single ply flake/vinyl ester tensile specimen

As seen in Figure 26, strain is not uniform throughout the volume of the specimen as it would be in an isotropic specimen. Strain increases much more on the left side of the specimen than on the right side, and is highest in two specific regions. The crack initiates at a region of high strain and the strain remains very high at the tip of the crack as it grows from left to right. The crack would

have been expected to initiate in the specimen at the first high strain region that develops near the top of the specimen area shown. However, this region of high strain may have been a surface effect or an area where the paint cracked but the specimen did not. Many localized regions of high strain are expected due to the morphology of the flake laminates. High stress concentrations would be expected to develop at the edges and corners of each flake. These effects should be mitigated to fabricate stronger laminates.

3.10 Tensile Failure Modes of Single Ply Flake/Vinyl Ester Laminates

As seen in Figure 27 below, the failure surfaces of the tension specimens are nearly identical to those of the flexure specimens and show that disbonding was the dominant failure mode. All images were taken at an original magnification of 3.75X.

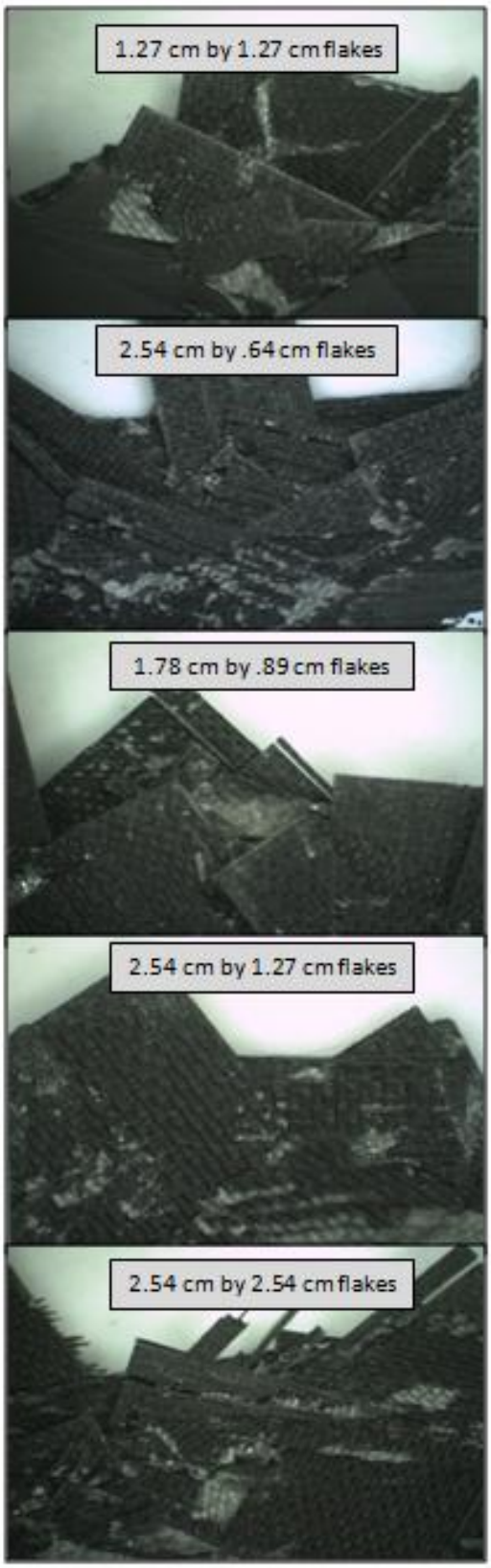

Figure 27: Fracture surfaces of single ply flake/vinyl ester tensile specimens

The disbonding shown in Figure 26 and the absence of broken flakes or fibers in most specimens is very undesirable because the fibers were not utilized to their maximum capability. Higher strength could have been achieved by using a resin system that bonded better to the flakes and by using longer flakes. Optimum flake length will be discussed in section 3.14.

Although disbonding was the dominant failure mode observed in the tensile specimens, additional orientation-dependent failure modes were observed as well. The tensile specimens from each laminate with the highest strengths tended to have failure surfaces with more exposed flakes oriented 45 degrees or more to the loading direction. The lower strength specimens tended to have failure surfaces with more exposed flakes oriented at low angles to the loading direction. These flakes experienced cracking in the fiber direction, as expected. An example of this type of cracking in a tensile specimen from the single ply flake/vinyl ester laminate fabricated with 2.54 cm by .64 cm (1 in by .25 in) flakes is shown below in Figure 28. The image was taken at an original magnification of 3.75X.

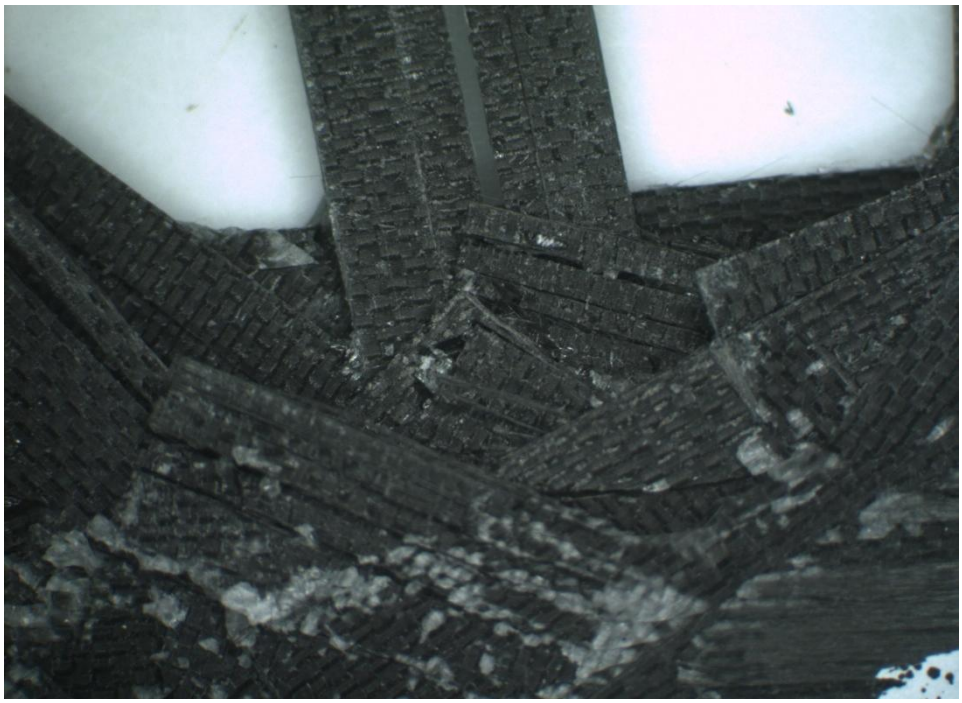

Figure 28: Cracking along the fiber direction in low-angle flakes

Flake cracking in the fiber direction was the expected failure mode for flakes oriented at low angles to the loading direction. However, the differences in prevalent flake orientations between the strongest and weakest specimens from the laminates casts doubt on the degree of randomness we achieved when scattering the flakes in the mold. Ideally, the flakes should have been oriented completely randomly with no prevalent orientation in any direction. It may be that the low strength laminates failed at localized regions of low strength where the fibers were prevalently oriented at low angles to the loading direction. More consistent processing is needed, as mentioned in section 3.5.

3.11 Analysis of the Data Scatter in the Measured Mechanical Properties of Single Ply Flake/Vinyl Ester Laminates

As seen in the error bars shown in Figures 20, 21, and 23, the data scatter for flexural and tensile properties was very large. Table 3 below quantifies the degree of scatter in the data by presenting the coefficient of variation (CV) for each test. The coefficient of variation is the ratio of the standard deviation of a data set to the average of that data set. Thus, it gives a measure of the degree of scatter in a data set.

Table 3: Coefficients of variation for flexural and tensile properties of the single ply flake/vinyl ester laminates

Mechanical Property	Flake Type	Flake Size (in by in)	CV (%)
Flexural Strength	Single Ply	.5 x .5	24.3
	Single Ply	1 x .25	31.9
	Single Ply	.7 x .35	15.7
	Single Ply	1 x .5	18
	Single Ply	1 x 1	33.1
	Shredded	N/A	2.3
Flexural Modulus	Single Ply	.5 x .5	17.9
	Single Ply	1 x .25	22.7
	Single Ply	.7 x .35	11.2
	Single Ply	1 x .5	11.4
	Single Ply	1 x 1	20.6
	Shredded	N/A	3.7
Tensile Strength	Single Ply	.5 x .5	8.9
	Single Ply	1 x .25	6.4
	Single Ply	.7 x .35	13.5
	Single Ply	1 x .5	27.7
	Single Ply	1 x 1	18.3
	Shredded	N/A	16.1

As seen in Table 3, CV values were very high among all the laminates, regardless of which mechanical test was performed. CV values were typically highest for the flexural strengths of the single ply flake/vinyl ester laminates. This was expected since only a small region of the specimen is subjected to the maximum load during three point bending and the distribution of flaws can greatly affect the strength values among different specimens. CV values for tensile properties were expected to be lower since the entire volume of the specimen, and hence all its flaws, are subjected to the maximum load during a tensile test. The CV values for modulus were expected to be lower than for strength. However, this was not true for tension.

Even though the CVs for the mechanical properties of single ply flake/vinyl ester laminates are higher than desired, they comparable well to the CVs for the mechanical properties of other flake reinforced materials. For the prepreg-based discontinuous carbon fiber/epoxy system described in section 1.6, the tensile modulus CVs ranged from 12 to 19% *(34)*. The tensile modulus CVs of the single ply flake/vinyl ester laminates ranged from 10-24%, and only one laminate had a

tensile modulus CV above 19%. For the tensile strength of a particular southern pine/phenol resin OSB, the CV was 23% *(35)*. The tensile strength CVs of the single ply flake/vinyl ester laminates were between 6 and 28%, and only one laminate a tensile strength CV above 23%. These comparisons indicate that high scatter and variability are an inherent characteristic of flake reinforced laminates and are not necessarily an indicator of poor processing. Nonetheless, there is still potential to reduce data scatter from our laminates through better processing and test methods.

As mentioned in section 3.5, flake packing in some regions of the single ply flake/vinyl ester laminates was very poor. A consistently high flake packing would likely improve CV values as well as overall mechanical properties. It is also possible that there are regions where flake orientation is not completely random. Even with high flake packing, small regions with aligned flakes would have different local properties that would also significantly contribute to data scatter in measured mechanical properties. For flake reinforced composites, more than 5 specimens per sample should be tested to help account for the inherently high variability in properties, reduce the CVs, and obtain more statistically significant data.

3.12 Evaluation of the Mechanical Properties of Single Ply Flake/Vinyl Ester Laminates

Table 4 below provides a comparison between the flexural and tensile properties of the single ply flake/vinyl ester laminate fabricated with 2.54 cm by .64 cm (1 in by .25 in) flakes and those of several other types of laminates. This single ply flake/vinyl ester laminate was chosen for comparison because it had some of the best flexural and tensile performance of all the single ply flake/vinyl ester laminates.

Table 4: Mechanical property comparison between a single ply flake/vinyl ester laminate and several other types of laminates

	Tensile Strength (MPa)	Tensile Modulus (GPa)	Flexural Strength (MPa)	Flexural Modulus (GPa)
HexMC®/C/2000/R1A *(36)*	300	40	400	30
Prepreg-Based Discontinuous Carbon Fiber/Epoxy System *(29)*	241	45	586	24
Recycled Random Laminate: T300/Epoxy *(37)*	210	29	320	23
Recycled Random Laminate: T700/Epoxy *(38)*	197	29	365	N/A
Single Ply Flake/Vinyl Ester Laminate: 2.54 cm by .64 cm Flakes	71	15	173	18

In Table 4 above, the flexural and tensile properties of a single ply flake/vinyl ester laminate are compared with those of two other recycled laminates, HexMC®, and the Feraboli group's prepreg-based discontinuous carbon fiber/epoxy system. HexMC® was included because it represents the maximum achievable properties of a flake reinforced carbon fiber/epoxy material. The recycled laminates were included so that a single ply flake/vinyl ester laminate could be compared with recycled laminates fabricated by other methods. The T300/epoxy laminate was fabricated by reclaiming fibers from prepreg scrap with a thermo/chemical process and then compression molding the fibers with resin films. The T700/epoxy laminate was fabricated by reclaiming the fibers from a cured laminate using acid digestion and then infusing the reclaimed fibers with resin using VARTM. The properties of the recycled laminates given in Table 3 are the highest properties achieved by any of the T300/epoxy or T700/epoxy laminates fabricated during their respective studies.

In general, the mechanical properties of the single ply flake/vinyl ester laminates are far inferior to the mechanical of other recycled CFRP laminates, which are substantially lower than those of HexMC®. No flexural or tensile properties of a single ply flake/vinyl ester laminate met or exceed those of any other material compared.

Table 5 below provides a comparison between the flexural and tensile properties of the single ply flake/vinyl ester laminate fabricated with 2.54 cm by .64 cm (1 in by .25 in) flakes and those of cured vinyl ester resin and a glass chopped strand mat/vinyl ester lamiante.

Table 5: Mechanical property comparison between a single ply flake/vinyl ester laminate, cured vinyl ester, and a glass chopped strand mat/vinyl ester laminate

	Tensile Strength (MPa)	Tensile Modulus (GPa)	Flexural Strength (MPa)	Flexural Modulus (GPa)
Single Ply Flake/Vinyl Ester Laminate: 2.54 cm by .64 cm Flakes	71	15	173	18.5
Cured Vinyl Ester Resin *(39)*	84	3.1	134	4.2
Chopped Strand Mat/Vinyl Ester Laminate with 27.6% Glass Content *(39)*	137	11.5	159	6.9

As seen in Table 5, we did not achieve adequate reinforcement of the vinyl ester with the single ply flakes. Although the tensile and flexural moduli and the flexural strength of the single ply flake/vinyl ester laminate are all higher than those of cured vinyl ester resin and the chopped strand mat laminate, the tensile strength is lower. The mechanical properties of recycled CFRP composite must be greater than those of random short fiber glass composites fabricated with virgin fibers if a recycled material is to be used instead. Ideally, recycled CFRP would be able to perform as well as a random short fiber CFRP laminate fabricated with virgin fibers.

Although our recycled laminates had poor mechanical performance, this was primarily due to the poor bonding between the flakes and the matrix, as emphasized in sections 3.7 and 3.10. This problem could likely be alleviated by choosing a more compatible resin system, using a different surface preparation method for the flakes, and optimizing flake geometry by increasing flake length.

3.13 Evaluation of the Tensile Properties of Shredded Flake/Vinyl Ester Laminates

Figure 29 below compares the tensile strength of the 25.4 cm by 25.4 cm (10 in by 10 in) shredded flake/vinyl ester laminate with the tensile strengths of the single ply flake/vinyl ester

laminates fabricated with the best and worst single ply flake geometries. The best flake geometry was the flake geometry used in the laminate with the highest tensile strength of all the single ply flake/vinyl ester laminates. The worst flake geometry was the flake geometry used in the laminate with the lowest tensile strength of all the single ply flake/vinyl ester laminates. The best flake geometry was 2.54 cm by .64 cm (1 in by .25 in), while the worst flake geometry was 1.79 cm by .89 cm (.7 in by .35 in). Although these were the best and worst flake geometries with respect to tensile properties, they were not the best and worst flake geometries with respect to flexural properties.

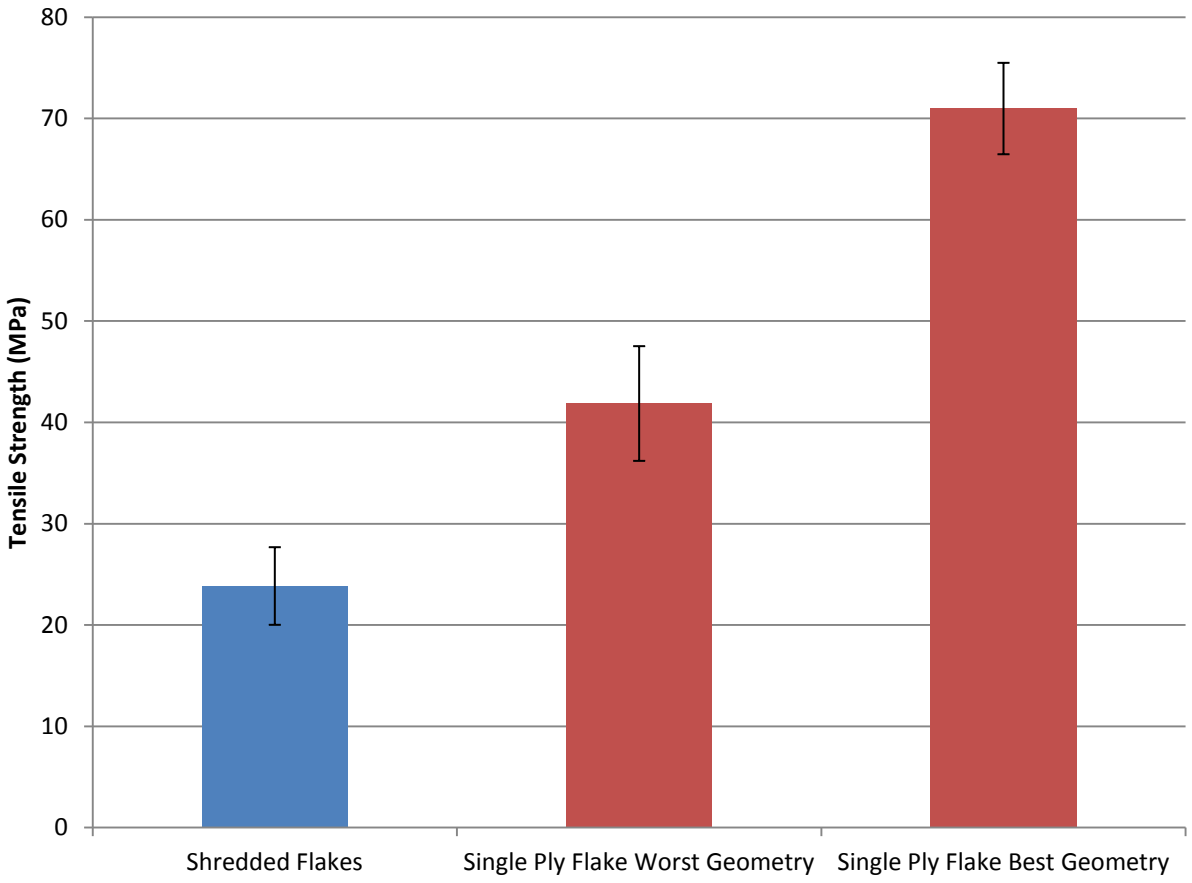

Figure 29: Flexural and tensile properties of the shredded flake/vinyl ester laminate

The tensile strength of the shredded flake laminate was much lower than the tensile strengths of the single ply flake vinyl/ester laminates fabricated with flakes of the best and worst geometries. The tensile strength of single ply flake/vinyl ester laminate fabricated with flakes of the best

geometry was more than twice that of the shredded flake/vinyl ester laminate. The flexural properties of the shredded flake/vinyl ester laminate were poor as well.

The comparatively low mechanical properties of the shredded flake laminates can likely be attributed to relatively small flake surface area to flake volume ratios and cracking induced in the matrix during the shredding process. In comparison to the single ply flakes, the shredded flakes had much less surface area per volume for bonding with the matrix. Although the cracks were fully infused with the secondary matrix resin, the crack tip would still act as a significant stress concentrator. These stress concentrations may have split the flakes at a relatively low applied stress. This is supported by the tensile failure mode of the shredded flakes. Unlike the single ply flakes, which completely disbonded from the vinyl ester matrix with no observed flake or fiber damage, the shredded flakes experienced fracture through the flakes, as well as disbonding. A typical flake fracture surface from a specimen tested in tension is seen below in Figure 30. The image was taken at an original magnification of 3.75X.

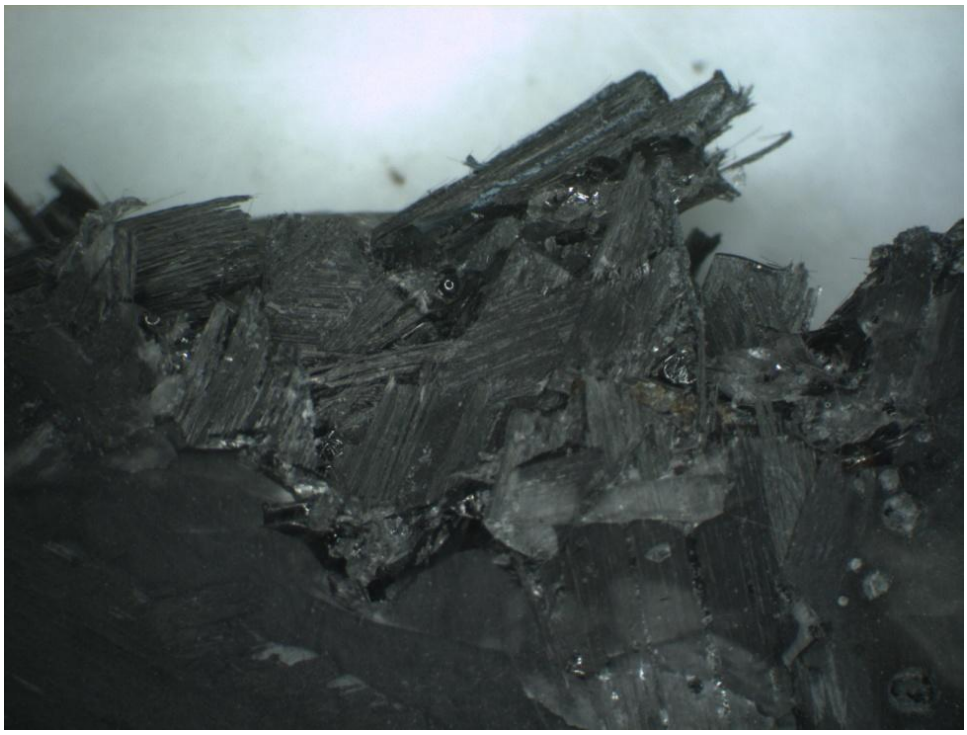

Figure 30: Typical fracture surface of a shredded flake/vinyl ester tensile specimen

It is difficult to tell whether fracture surface characteristics such as fiber failure and flake damage originated during the shredding process or during failure of the tensile specimens. However, comparison of the two matching fracture surfaces of each shredded flake/vinyl ester tensile specimen shows that failure typically occurred within the flakes. Some disbonding occurred as well. This can be seen in Figure 31 below, which shows the imprint of flake fibers in a fragment of resin present on a fracture surface of a shredded flake/vinyl ester tensile specimen. The image was taken at an original magnification of 35X.

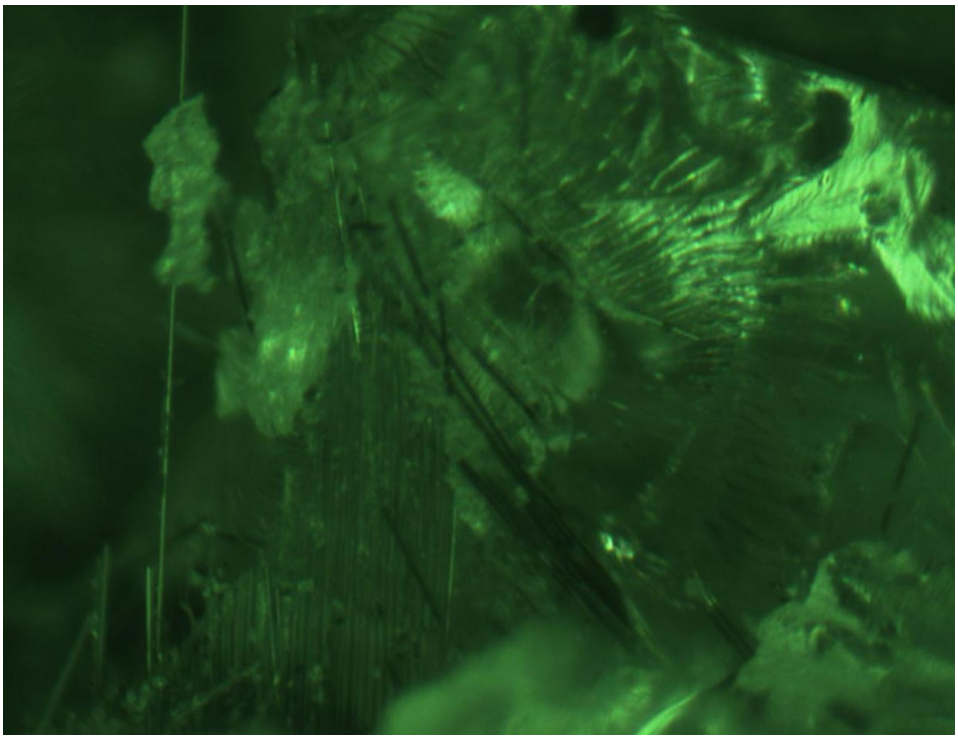

Figure 31: Imprint of shredded flake fibers in a fragment of resin present on the fracture surface of a shredded flake/vinyl ester tensile specimen

3.14 Development and Evaluation of a Shear-Lag Model for Flake Reinforced Composites

Based on the model given in section 1.5, a similar shear-lag model can be developed for flake reinforced laminates. Application of this model to our single ply flake/vinyl ester laminates further illustrates the need for optimized flake geometry and better bonding between the flakes and the matrix. In the following analysis, the subscript "F" denotes a variable for a flake rather

than a fiber. As in Figure 3, force equilibrium on an infinitesimal length of flake can only occur if shear stress is present at the fiber matrix interface, as shown below.

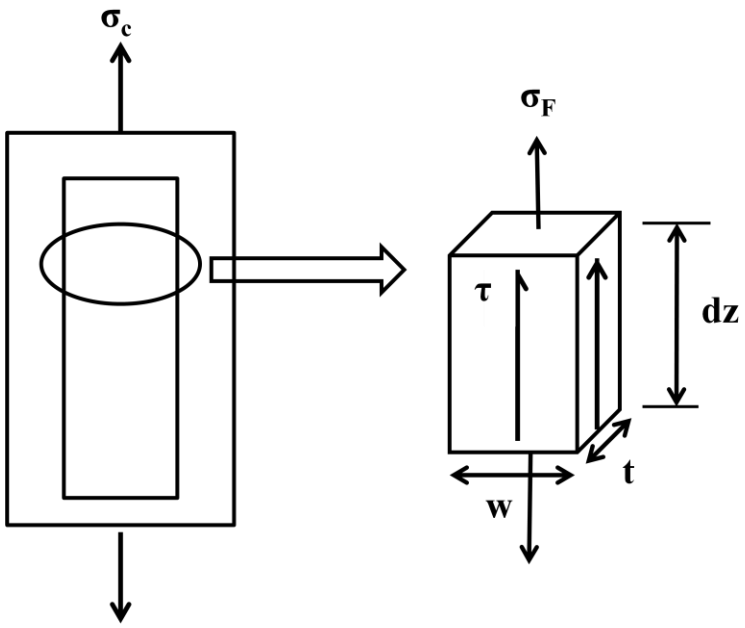

Figure 32: Equilibrium of a small length of flake in a flake reinforced composite

Force balance on a small length of flake yields:

$$\sigma_F(tw) + 2\tau dz(w+t) = (\sigma_F d\sigma_F)tw \qquad \text{[Equation 10]}$$

Rearrangement of Equation 10 yields:

$$\frac{d\sigma_F}{dz} = \frac{2\tau(w+t)}{tw} \qquad \text{[Equation 11]}$$

Integration of Equation 11 yields the force in the flake a distance z away from the flake end:

$$\sigma_F = \sigma_{F0} + \frac{2\tau(w+t)}{tw}\int_0^z \tau\, dz \quad \text{[Equation 12]}$$

Neglecting the stress in the flake end and assuming the matrix is perfectly plastic so that the interfacial shear stress is constant along the fiber length, integration of the force balance yields:

$$\sigma_F = \frac{2\tau(w+t)}{tw} \quad \text{[Equation 13]}$$

Assuming the stress in a short flake increases linearly from each and reaches a maximum at the midlength of the flake like it does in a short fiber:

$$\sigma_{F,max} = \frac{l\tau(w+t)}{tw} \quad \text{[Equation 14]}$$

Rearrangement of Equation 15 gives the load transfer length:

$$l_t = \frac{\sigma_{F,max}tw}{(w+t)\tau} \quad \text{[Equation 16]}$$

The maximum possible stress in the flake is equal to the ultimate stress of a continuous unidirectional laminate fabricated from the same material, or $\sigma_{F,ultimate}$. The minimum flake length in which the maximum allowable flake stress can be achieved is thus given by:

$$l_c = \frac{\sigma_{F,ultimate} t w}{(w+t)\tau} \qquad \text{[Equation 17]}$$

This equation gives the critical length for an aligned discontinuous laminate reinforced with rectangular flakes. The critical length shows only a small dependence on w for a fixed t , just as the mechanical properties of the single ply flake/vinyl ester laminates showed essentially no variation with increasing flake width for flakes of a constant width and thickness.

In Equation 17, the ultimate stress of the flake, $\sigma_{F,ultimate}$, can be determined from tensile tests of the material the flakes originated from. τ is either the yield strength of matrix in shear or the flake-matrix bond strength in shear, whichever is lower. This can also be determined for most material systems.

For the single ply flakes used in this study, $\sigma_{F,ultimate}$, is equal to the ultimate strength of the unidirectional T800S/3900-2 system in the 0 direction: 2,950 MPa. The thickness,t, is equal to the approximate thickness of a single ply of T800S/2900-2: .2 mm (.008 in). Substituting these values into Equation 17 gives:

$$l_c = \frac{(2950).2w}{(w+.2)\tau} \qquad \text{[Equation 18]}$$

τ is often approximated as the matrix yield strength in shear, τ_y. However, this is only a valid approximation if perfect flake-matrix bonding is achieved. Since disbonding was the predominant failure mode of the single ply flake/vinyl ester laminates in tension, we know that the actual τ for this material system was much lower than τ_y. We can get an idea of what the actual critical flake length would be for our material system by plotting the critical flake length versus flake width as τ decreases from its maximum possible value of τ_y to lower values that represent systems with poor fiber-matrix bonding.

τ_y can be approximated as $\frac{\sigma_{UTS}}{2}$. For the vinyl ester used in this study, σ_{UTS} = 84 MPa, so τ_y can be approximated as 42 MPa. Figure 33 below shows how the critical flake length for a single ply flake/vinyl ester system changes with increasing flake length as the fiber-matrix bond strength decreases from its approximate maximum value of 42 MPa.

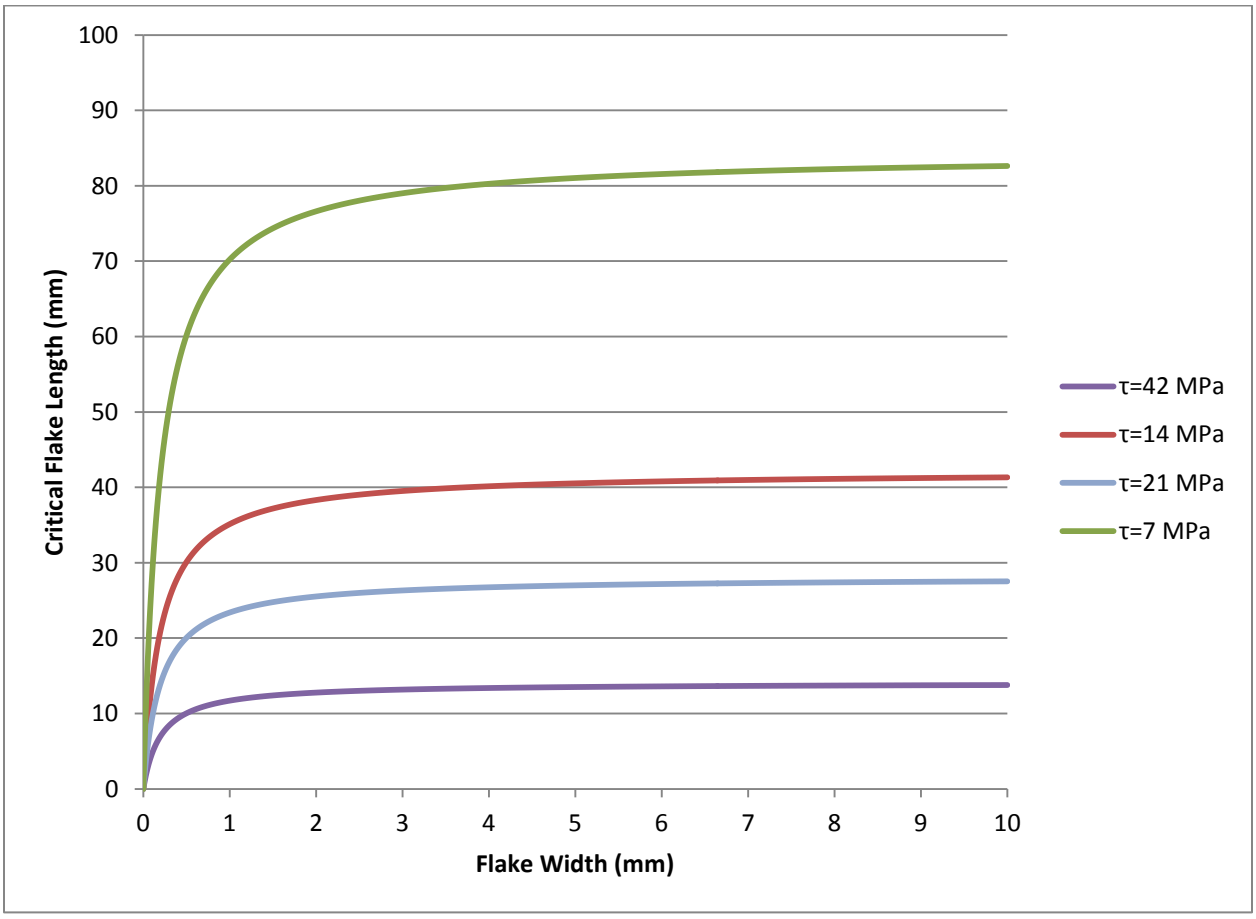

Figure 33: Critical flake length versus flake width for an aligned single ply flake/vinyl ester laminate as τ decreases

As seen in Figure 33, the critical length increases rapidly as width increases and then levels off. The critical length reaches a plateau value at shorter flake widths for laminates with better flake-matrix bonding (higher values of τ). For a single ply flake/vinyl ester laminate with perfect flake-matrix bonding ($\tau = 42\ MPa$) the critical flake length increases from .67 mm to 13.77 mm as flake width increases from .01 mm to 10 mm. Therefore, assuming that all flakes would be at

least 10 mm long, the shortest possible critical flake length for an aligned single ply flake/vinyl ester laminate with perfect flake-matrix bonding is 13.77 mm. This is significantly longer than critical length of only .05 mm for a T800S fiber with an ultimate strength of 5,880 MPa in epoxy if τ is approximated as 28 MPa *(21, 33)*.

For a laminate with extremely poor flake-matrix bonding ($\tau = 7\ mm$), the critical flake length increases from 4.01 mm to 82.63 mm as flake width increases from .01 mm to 10 mm. The critical flake length for the single ply flake/vinyl ester system is thus between 13.77 mm and 82.63 mm, and likely much closer to the lower bound since disbonding was the predominant tensile failure mode. Furthermore, these bounds are only for an aligned material system so the actual critical flake length would be longer than that calculated using Equation 18. Since we did not see any flake failure in our single ply flake/vinyl ester laminates, we also know that the critical flake length must be longer than 25.4 mm, which was the longest flake length we used in this study. Based on these results, we need to choose a more compatible resin system, increase flake length, or both.

3.15 Rule of Mixtures Prediction of the Flexural Modulus of Single-Ply Flake-Vinyl Ester Laminates

For an aligned single ply flake vinyl/ester laminate fabricated with 1.27 cm by 1.27 cm (.5 in by .5 in flakes), the experimental flexural modulus agrees well with that predicted from the longitudinal rule of mixtures when the flexural modulus of the fiber is replaced by the flexural modulus of a unidirectional T800S/3900-2 laminate in Equation 3. This is shown below in Figure 34.

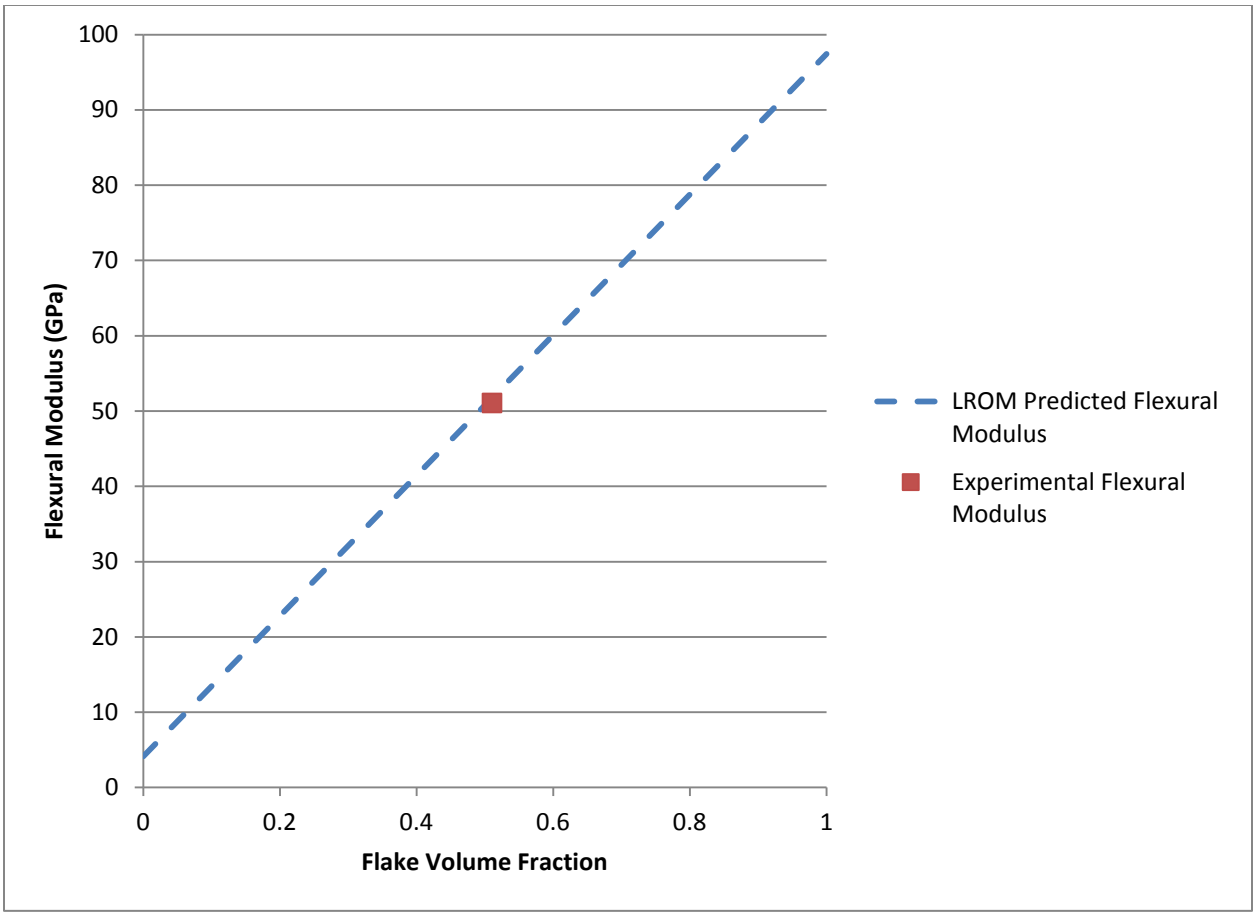

Figure 34: Predicted and experimental flexural modulus of an aligned single ply flake/vinyl ester laminate

As seen in Figure 34, the experimental flexural modulus is nearly the same as that predicted by the longitudinal rule of mixtures. Testing of aligned laminates with different volume fractions would be needed to completely verify this model. However, the single data point shown in Figure 34 still provides evidence that the properties of flake reinforced laminates can likely be predicted with slightly modified models used to predict the properties of other types of composites.

For random single ply flake/vinyl ester laminates, the values of the experimental moduli fall in between those predicted by the LROM and the TROM when the modulus of the fiber is replaced with the modulus of a quasi-isotropic $[0/45/90/-45]_{4S}$ T800S/3900-2 laminate in Equations 3 and 4 . This is shown in Figure 35 below.

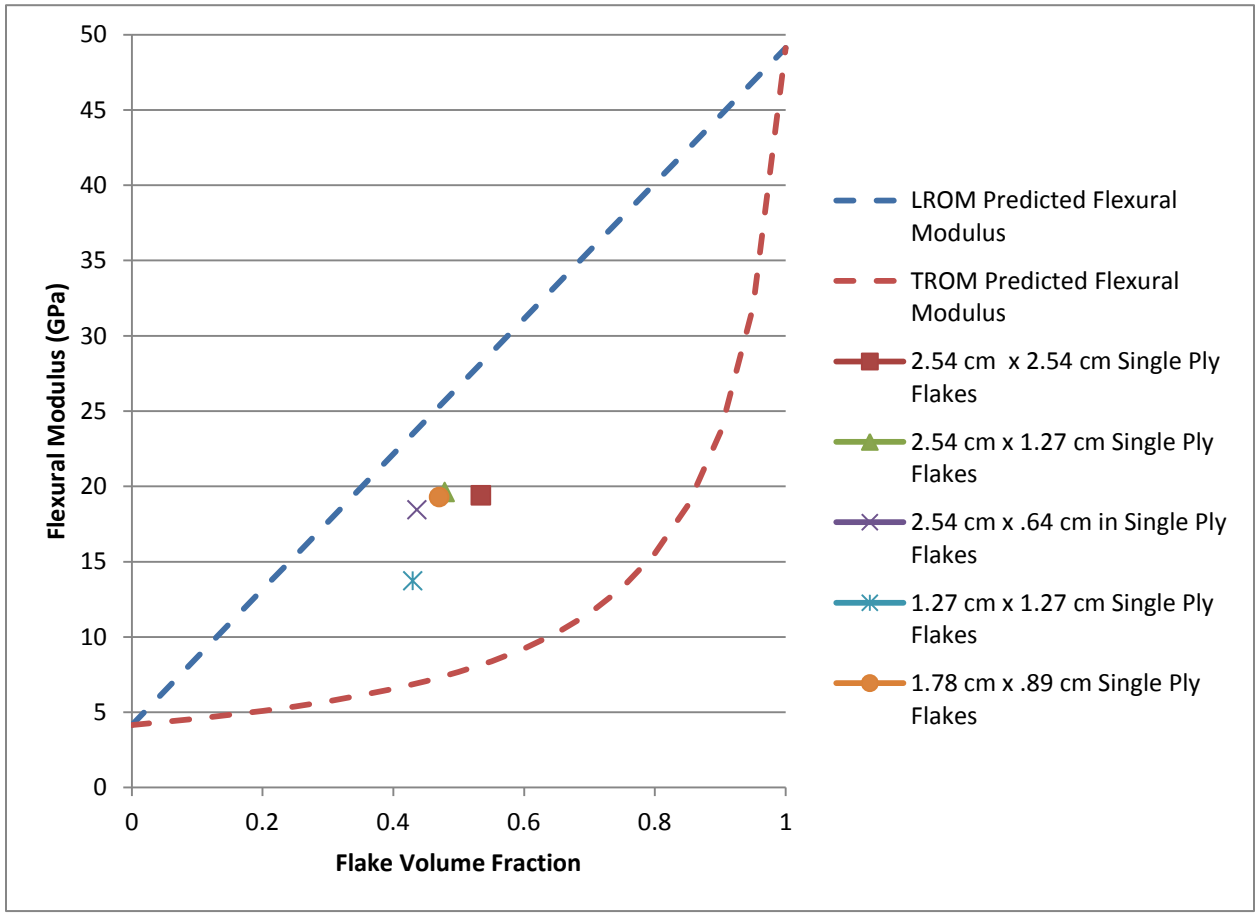

Figure 35: Predicted and experimental flexural moduli of random single ply flake/vinyl ester laminates

Figure 35 further supports the idea that the models used to predict the properties of short fiber laminates could be modified to accurately predict the properties of random flake reinforced laminates. In general, random short fiber composites are expected to have modulus values closer to those predicted by the TROM, as evidenced in Equations 7 and 8. Our values are closer to the LROM prediction because of the assumption of randomness we made in using the flexural modulus of a quasi-isotropic T800S/3900-2 laminate as E_f in Equations 3 and 4.

The agreement between the predicted and experimental moduli of single ply flake/vinyl ester laminates is especially promising because our laminates were not ideally fabricated. Processing improvements that reduce porosity and increase the uniformity of the flake distribution may yield even better agreement between the experimental and predicted values of the flexural

moduli of these laminates. Since the models assume perfect bonding between the matrix and the fibers, single ply flake laminates fabricated with a different resin would be expected to fit the LROM model better than our current laminates. It also possible that a more elaborate model such as one based on the Halpin-Tsai model would be required for more accurate predictions. Additional aligned laminates with different flake volume fractions would need to be fabricated and tested in both the longitudinal and transverse directions in order to see if equations 7 or 8 could be used with the Halpin-Tsai equations to accurately predict the tensile and flexural properties of a random single ply flake/vinyl ester laminates. As with the LROM equation, the Halpin Tsai equations would be modified to include flake moduli rather than fiber moduli.

Chapter 4: Conclusion

The goal of this research was to investigate the effect of flake geometry on the properties of recycled flake reinforced composites and to evaluate whether fabricating recycled laminates with CFRP flakes has potential as a viable alternative to current CFRP recycling techniques. This was accomplished by fabricating and testing flake reinforced laminates with two different types of flakes with vastly different geometries: shredded flakes and single ply flakes. The geometry of the single ply flakes was also varied while holding either flake area or flake length constant.

We first characterized the reinforcement to gain a proper understanding of our starting geometries. The shredded flakes were shown to have significant microcracking caused by the shredding process, while the single ply flakes showed nearly no damage caused by manufacturing.

We initially fabricated several 15.2 cm by 15.2 cm (6 in by 6 in) laminates and tested them in flexure. Single ply and shredded flake reinforced laminates fabricated with vinyl as the matrix showed similar flexural performance to comparable laminates fabricated with epoxy as the matrix. For the shredded flake reinforced laminates, the presence of fines in the flakes was shown to have little effect on flexural properties.

Next we fabricated larger 25.4 cm by 25.4 cm (10 in by 10 in) laminates and tested them in both flexure and tension. For single ply flake/vinyl ester laminates, flexural strength, flexural modulus, and tensile strength were shown to increase with increasing flake area. However, this was attributed to an increase in flake length since the properties of all the single ply flake/vinyl ester laminates fabricated with 2.54 cm (1 in) long flakes were very similar, regardless of flake width. Digital image correlation showed that failure occurred at localized regions of high strain and provided an approximate value for the tensile modulus we can expect of our current single ply flake/vinyl ester laminates.

The tensile strengths of the single ply flake/vinyl ester laminates were far superior to the tensile strength of the shredded flake/vinyl ester laminate. The low mechanical properties of the shredded flake/vinyl ester laminate were attributed to the relatively low surface are to volume ratios of the shredded flakes and microcracking in the flakes caused by the shredding process.

In comparison to other recycled CFRP laminates, the performance of our recycled flake reinforced laminates was very poor. This was primarily attributed to poor bonding between the flakes and the matrix, as well as inconsistent flake packing and localized regions of high resin content. Flake lengths of 2.54 cm (1 in) were not adequate for our material system and did not yield a desirable tensile or flexural failure mode. However, flake length can be easily manipulated and poor bonding can be easily overcome in the future by choosing a different resin system and/or a different surface preparation for the flakes. The data scatter was also very high in all the measured mechanical properties, but can likely be reduced by improving the consistency of our fabrication process and by performing testing on a larger specimen population.

The future promise of flake reinforced laminates was perhaps best exemplified by the aligned single ply flake/vinyl ester laminate. We showed that we can achieve property values equal to the predicted values, at least for flexural modulus. Much future work is needed to verify whether the properties of flake reinforced laminates may be approximated by models already developed for short fiber composites. However, this result represents a significant step forward in understanding the mechanical behavior of flake reinforced composites. The flexural moduli of the random single ply flake/vinyl ester laminates were also within the expected range.

Despite the relatively poor mechanical properties of our recycled laminate, this study still provided valuable insight into the mechanical behavior and future potential of recycled flake reinforced laminates. Recycled laminates with cured CFRP flake reinforcement have not been fabricated before. Hence, everything we learned in this study represents progress towards understanding the mechanical behavior of this class of laminates and determining optimum flake geometry. We identified many of the problems that an optimal processing method must overcome, such as inconsistent flake distribution and orientation, and we now know that future laminates must have longer flake lengths and better flake-matrix bonding. This study will encourage future research in the field of CFRP recycling and ultimately contribute to better solutions for recycling CFRP waste.

Chapter 5: Future Work

This study was the first research we know of related to the properties of recycled laminates with cured CFRP flake reinforcement. Hence, there is a great deal of future work to be accomplished.

Most importantly, we need to determine a resin system that will bond well to T800S/3900-2 flakes so that we can fully utilize the properties of the high strength fibers. Different surface preparations for the single ply flakes and potential surface treatments for the shredded flakes should also be investigated to improve bonding. The critical flake length for each type of flake should be determined as well.

Automated processes for randomly scattering flakes should be investigated so that we can achieve more uniform flake packing and the highest possible degree of randomness. Continuous processes such as those used to fabricate OSB could possibly be modified to suit CFRP flakes. Alignment processes would also be worth investigating since we achieved a flexural modulus nearly equal to that predicted by the longitudinal rule of mixtures for the aligned single ply flake/vinyl ester laminate. Although aligned short fiber composites are used much less commonly than random short fiber composite, aligned flake composites may find a niche market similar to that of OSB where high bending stiffness and bending strength is required.

Flake and fiber volume fractions will need to be improved before we can achieve optimum properties with the CFRP flake reinforced laminates. Alternatives to VARTM such as compression molding should be investigated. The current VARTM process could also be improved to eliminate porosity in the laminates. Using CAPRI instead of VARTM would also be expected to improve laminate quality. Fabricating larger laminates would be desirable, but would require a more elaborate VARTM or CAPRI inlet tube configuration so that larger areas could be properly infused.

There are also many properties of recycled flake reinforced composites that have yet to be studied. The coefficient of thermal expansion of the flake reinforced laminates should be investigated to determine whether recycled flake reinforced laminates would be suitable tooling materials. Compressive and shear properties should be determined as well. We would also like to investigate whether test specimen geometry has an effect on measured properties, such as if measured tensile properties differ when thicker or wider specimens are tested.

REFERENCES

1. Pimenta, S.; Pinho, S.T. Recycling Carbon Fibre Reinforced Polymers for Structural Applications: Technology Review. *Waste Manage.* **2011,** *31,* 378-392.

2. Pickering, S., J. Recycling Technologies for Thermoset Composite Materials-Current Status. *Compos. Part A-Appl. S.* **2006,** *37,* 1206-1215.

3. Wong, K.H.; Pickering, S.J.; Turner, T.A.; Warrior, N.A. Compression Moulding of a Recycled Carbon Fibre Reinforced Epoxy Composite. In *SAMPE 2009,* Baltimore, Maryland, May 18-21, 2009; Society for the Advancement of Material and Process Engineering. http://sampe.org (accessed Nov 7, 2011).

4. Wong, K.H.; Pickering, S.J.; Turner, T.A.; Warrior, N.A. Alignment of Discontinuous Recycled Carbon Fibre. In *SAMPE 2011,* Long Beach, California, May 23-26, 2011. Society for the Advancment of Material and Process Engineering. http://sampe.org (accessed Nov 7, 2011).

5. Conroy, A.; Halliwell, S.; Reynolds, T. Composite Recycling in the Construction Industry. *Compos. Part A-Appl. S.* **2006,** *37,* 1216-1222.

6. Hurley, K.H.; George, P.E. Carbon Fiber Recycling: Optimizing Fiber Volume Fraction in Recycled Short-Fiber Laminates. In *SAMPE 2011,* Long Beach, California, May 23-26, 2011. http://sampe.org (accessed Nov 7, 2011).

7. Kouparitsas, C.E.; Kartalis, C.N.; Varelidis, P.C.; Tsenoglou, C.J.; Papaspyrides, C.D. Recycling of the Fibrous Fraction of Reinforced Thermoset Composites. *Polym. Composite.* **2002,** *23,* 682-689.

8. *Wood Particleboard and Flakeboard Types, Grades, and Uses*; FPL-GTR-53; U.S. Department of Agriculture, Forest Service, Forest Products Laboratory: 1986.

9. *Oriented Strand Board and Waferboard;* Structural Board Association technical bulletin No. 103. Markham, Ontario, Canada.

10. OSB Guide. OSB Performance By Design Manual: Oriented Strand Board in Wood Frame Construction." http://osbguide.tecotested.com/osbliterature_en (accessed Nov 7, 2011).

11. Stark, N.M.; Cai, Z., & Carll, C. G. *Wood Handbook, Chapter 11: Wood-Based Composite Materials-Panel Products- Glued-Laminated Timber, Structural Composite Lumber, and Wood-Nonwood Composite Materials*. FPL-GTR-190; U.S. Department of Agriculture, Forest Service, Forest Products Laboratory: Madison, WI, 2010.

12. Haughton, L.;Murphy, C. Moisture Exchange: Performance of OSB and Plywood Structural Panels. *Interface*, June 2003, pp 6-13.

13. *Binders and Waxes in OSB*; Structural Board Association technical bulletin No. 114. Markham, Ontario, Canada.

14. Gunduz, G.; Yapici, F.; Ozcifci, A.; Kalaycioglu, H. The Effects of Adhesive Ratio and Pressure Time on Some Properties of Oriented Strand Board. *BioResources* **2011,** *6*, 2118-2124.

15. Post, P.W. Effect of Particle Geometry and Resin Content on Bending Strength of Oak Flake Board, *Forest Prod. J.* **1958,** *10*, 317-322.

16. Post, P.W. Relationship of flake size and resin content to mechanical and dimensional properties of flakeboard. *Forest Prod. J.* **1961,** *11,* 34-37.

17. Brumbaugh, J. Effect of flake dimensions on properties of particleboards. *Forest Prod. J.* **1960,** *40*, 55-62.

18. Suzuki, S.; Takeda, K. Production and Properties of Japanese Oriented Strand Board I: Effect of Strand Length and Orientation on Strength Properties of Sugi Oriented Strand Board. *J. Wood Sci* **2000,** *46*, 289-295.

19. Laufenberg, T. L. Flakeboard Fracture Surface Observations and Correlation with Orthotropic Failure Criteria *J. I. Wood Sci.* **1984,** *10,* 57-65.

20. Rosen, W. Mechanics of Composite Strengthening. Presented at *The ASM Seminar on Fiber Composite Materials*, Philadelphia, Pennsylvania, October 17, 1964. American Society for Metals, Metals Park, OH.

21. Agarwal, B.D.; Broutman, L.J.; Chandrashekhara, K. *Analysis and Performance of Fiber Composites*, 3rd Ed.; John Wiley & Sons: Hoboken, NJ, 2006.

22. Lu, Yunkai. Mechanical Properties of Random Discontinous Fiber Composites Manufactured from Wetlay Process. M.S. Thesis, Virginia Polytechnic Institute and State University, Blacksburg, VA, 2002.

23. Halpin, J.C.; Kardos, J.L. The Halpin-Tsai Equations: A Review. *Polym. Eng. Sci.* **1976,** *16,* 344-352.

24. Kardos, J.L. Critical Issues in Achieving Desirable Mechanical Properties for Short Fiber Composites. *Pure Appl. Chem.* **1985,** *57,* 1651-1657.

25. Shaler, S.M.; Blankenhorn, P.R. Composite Model Prediction of Elastic Moduli for Flakeboard. *Wood Fiber Sci.* **1990,** *22,* 246-261.

26. Blizard, K.; Portway, J. A Wholly Recycled Structural Plastic Lumber Incorporating Scrap Prepreg Waste. In *ANTEC '97: Proceedings of ANTEC '97*. Toronto, Ontario, Canada, April 27-May 2, 1997. Society of Plastics Engineers; pp. 3141-3145.

27. Fudge, Jack. HexMC™- Composites in 3D. In *SAMPE 2011*, Long Beach, California, May 6-10, 2001. http://sampe.org (accessed Nov 7, 2011).

28. Hexcel. HexMC® User Guide2008. http://www.hexcel.com/Resources/UserGuides/HexMC_UserGuide.pdf (accessed Nov 7, 2011).

29. Feraboli, P.; Peitso, E.; Deleo, F.; Cleveland, T. Characterization of Prepreg-Based Discontinuous Carbon Fiber/Epoxy Systems. *J. Reinf. Plast. Comp.* **2009,** *28,* 1191-1214.

30. ASTM Standard D790-10, 2010. "Standard Test Methods for Flexural Properties of Unreinforced and Reinforced Plastics and Electrical Insulating Materials." ASTM International, West Conshohocken, PA, 2010, www.astm.org.

31. ASTM Standard D3039/D3039M-08, 2008. "Standard Test Method for Tensile Properties of Polymer Matrix Composite Materials". ASTM International, West Conshohocken, PA, 2008, www.astm.org.

32. ASTM D792-08, 2008. "Standard Test Methods for Density and Specific Gravity (Relative Density) of Plastics by Displacement." ASTM International, West Conshohocken, PA, 2008, www.astm.org.

33. Toray Carbon Fibers America, Inc. TORAYCA® T800S Data Sheet No. CFA-019. http://www.toraycfa.com/pdfs/T800SDataSheet.pdf (accessed Feb 25, 2012).

34. Feraboli, P.; Peitso, E.; Cleveland, T. Modulus Measurement for Prepreg-Based Discontinuous Carbon Fiber/Epoxy Systems. *J. Reinf. Plast. Comp.* **2009,** *43,* 1947-1965.

35. Wang, Y.; Young, T.M.; Guess, F.M.; Leon, R.V. Exploring Reliability of Oriented Strand Board's Tensile and Stiffness Strengths. *Int. J. Reliab.* **2007,** *8,* 111-124.

36. Hexcel. HexMC® Moulding Concept Carbon Epoxy HexMC®/C/2000/R1A. http://hexcel.com/Resources/DataSheets/Molding-Data-Sheets/R1A_wu.pdf (accessed Nov 7, 2011).

37. Janney, M.A.; Newell, W.L.; Geiger, E., Baitcher, N.; Gunder, T. Manufacturing Complex Geometry Composites with Recycled Carbon Fiber. In *SAMPE 2011*, Baltimore, Maryland, May 18-21, (2009). http://sampe.org (accessed Nov 7, 2011).

38. Feraboli, P.; Kawakami, H.; Wade, B.; Gasco, F.; DeOto, L.; Masini, A. Recyclability and Reutilization of Carbon Fiber Fabric/Epoxy Composites. *J. Compos. Mater.* **2011,** *0,* 1-15.

39. Fiberaly, Inc. Orca 511 Infusion V/E Resin. http://www.fiberlay.com/tech/55511D.PDF (acccessed Nov 7, 2011).